SEVEN-YEAR EVALUATION OF THREE INSTRUMENTED BRIDGE DECKS IN SACO, MONTANA

FHWA/MT-10-007/8204

Final Report

prepared for
THE STATE OF MONTANA
DEPARTMENT OF TRANSPORTATION

in cooperation with
THE U.S. DEPARTMENT OF TRANSPORTATION
FEDERAL HIGHWAY ADMINISTRATION

November 2010

prepared by
Eli Cuelho
Jerry Stephens
Michelle Akin

Western Transportation Institute
Montana State University - Bozeman

RESEARCH PROGRAMS

MDT

You are free to copy, distribute, display, and perform the work; make derivative works; make commercial use of the work under the condition that you give the original author and sponsor credit. For any reuse or distribution, you must make clear to others the license terms of this work. Any of these conditions can be waived if you get permission from the sponsor. Your fair use and other rights are in no way affected by the above.

SEVEN-YEAR EVALUATION OF THREE INSTRUMENTED BRIDGE DECKS IN SACO, MONTANA

Final Report

Prepared by:

Eli Cuelho, Jerry Stephens, and Michelle Akin

of the

Western Transportation Institute
College of Engineering
Montana State University – Bozeman

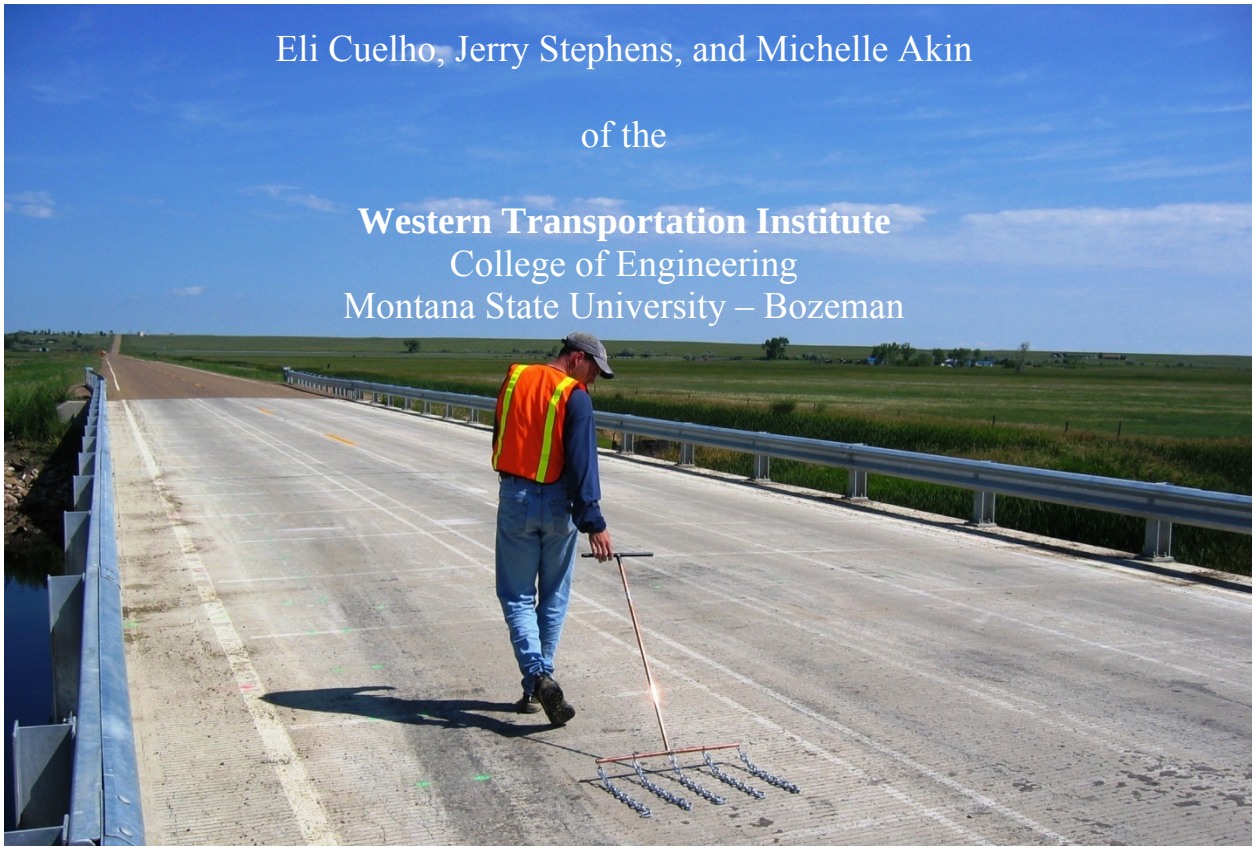

Prepared for:

Montana Department of Transportation
Research Programs
2701 Prospect Avenue
Helena, Montana 59620

November 2010

TECHNICAL REPORT DOCUMENTATION PAGE

1. Report No.	2. Government Access No.	3. Recipient's Catalog No.	
FHWA/MT-10-007/8204			
4. Title and Subtitle Seven-Year Evaluation of Three Instrumented Bridge Decks in Saco, Montana		5. Report Date November 2010 6. Performing Organization Code	
7. Author(s) Eli Cuelho, Jerry Stephens, and Michelle Akin		8. Performing Organization Report Code	
9. Performing Organization Name and Address Western Transportation Institute PO Box 174250 Montana State University – Bozeman Bozeman, Montana 59717-4250		10. Work Unit No. (TRAIS) 11. Contract or Grant No. MSU G&C #4W2781 MDT Project #8204	
12. Sponsoring Agency Names and Addresses Research Programs Montana Department of Transportation 2701 Prospect Avenue Helena, Montana 59620-1001		13. Type of Report and Period Covered Final Report August 2009 – November 2010 14. Sponsoring Agency Code 5401	
15. Supplementary Notes Research performed in cooperation with the Montana Department of Transportation and the U.S. Department of Transportation Research and Innovative Technology Administration. This report can be found at http://www.mdt.mt.gov/research/projects/structures/threedecks.shtml.			
16. Abstract Since the service life of concrete bridge decks designed by traditional procedures is often shorter than desired, their ability to withstand constant and heavy use in a variety of operating environments is of major concern. In this project, the relative performance of three bridge decks constructed with different concretes and reinforcing steel configurations was studied to help determine which deck offers the best performance over time. The decks investigated consist of a) a deck reinforced following the Montana Department of Transportation's (MDT's) standard practice constructed with conventional concrete, b) a deck reinforced according to AASHTO's empirical design procedure constructed with conventional concrete, and c) a deck reinforced following MDT's standard practice constructed with high performance concrete (HPC). The performance of the three decks was studied by conducting periodic visual distress surveys and corrosion tests and by monitoring data from an array of strain and temperature instrumentation embedded in each of the bridge decks during construction in 2003. The conclusion from an extensive evaluation conducted when the bridges were two years old indicated that the three bridge decks were generally behaving similarly. A follow-on evaluation when the bridges were seven years old revealed that the bridge decks continue to behave similarly, with the HPC deck possibly offering the best relative performance based on lower cracking levels and lower strain magnitudes. The decks are still relatively young, and more substantial differences in their durability and performance may emerge over time.			
17. Key Words Bridge deck instrumentation, long term monitoring, aging infrastructure, high performance concrete, durability, corrosion, field evaluation, strain measurements		18. Distribution Statement No restrictions. This document is available through NTIS, Springfield, Virginia 22161.	
19. Security Classif. (of this report) Unclassified	20. Security Classif. (of this page) Unclassified	21. No. of Pages 89	22. Price

DISCLAIMER STATEMENT

This document is disseminated under the sponsorship of the Montana Department of Transportation and the United States Department of Transportation in the interest of information exchange. The State of Montana and the United States Government assume no liability of its contents or use thereof.

The contents of this report reflect the views of the authors, who are responsible for the facts and accuracy of the data presented herein. The contents do not necessarily reflect the official policies of the Montana Department of Transportation or the United States Department of Transportation.

The State of Montana and the United States Government do not endorse products of manufacturers. Trademarks or manufacturers' names appear herein only because they are considered essential to the object of this document.

This report does not constitute a standard, specification, or regulation.

ALTERNATIVE FORMAT STATEMENT

MDT attempts to provide accommodations for any known disability that may interfere with a person participating in any service, program, or activity of the Department. Alternative accessible formats of this information will be provided upon request. For further information, call (406) 444-7693, TTY (800) 335-7592, or Montana Relay at 711.

ACKNOWLEDGMENTS

The authors would like to acknowledge the financial support for this project provided by the Montana Department of Transportation (MDT) and the Research and Innovative Technology Administration (RITA) at the United States Department of Transportation through the Western Transportation Institute at Montana State University. We also wanted to recognize and thank the MDT Research Section and the technical panel for their participation in this project. A final thank you goes to Jeff Johnson for his assistance during the site visits and help with the data analysis.

UNIT CONVERSIONS

Measurement	Metric	English
Length	1 cm	0.394 in
	1 m	3.281 ft
	1 km	0.621 mile
Area	1 cm^2	0.155 in^2
	1 m^2	1.196 yd^2
Volume	1 m^3	1.308 yd^3
	1 ml	0.034 oz
Force	1 N	0.225 lbf
	1 kN	0.225 kip
Stress	1 MPa	145 psi
	1 GPa	145 ksi
Unit Weight	1 kg/m^3	1.685 lbs/yd^3
Velocity	1 kph	0.621 mph

EXECUTIVE SUMMARY

While planning the replacement of three bridges on Montana Secondary Highway 243 north of Saco, Montana, bridge engineers at the Montana Department of Transportation (MDT) recognized and seized a unique opportunity to evaluate the performance of different deck designs exposed to the same vehicular and environmental loads. The new bridges have identical geometries, and were constructed at the same time (in 2003) by the same contractor, which helped minimize the number of variables typically encountered in large-scale field investigations of comparative performance. The primary focus of this research project has been to investigate the behavior of the three different deck designs (that have different concretes and reinforcing configurations) used in these bridges under long-term environmental exposure. The three different decks were:

1. a conventionally reinforced deck made with standard concrete (Conventional deck),
2. a deck with reduced reinforcement and standard concrete designed according to the American Association of State Highway and Transportation Officials (AASHTO) Load and Resistance Factor Design (LRFD) Bridge Design Specifications (Empirical deck), and
3. a conventionally reinforced deck made with high performance concrete (HPC deck).

An array of strain and temperature instrumentation was embedded in each of the bridge decks prior to placing the deck concrete. Long term monitoring consisted of measuring internal deck strains and temperatures, assessing corrosion potential, documenting visual distresses, and detecting global movement of the bridge structures through periodic topographic surveys of the bridge decks.

In 2006, a comprehensive report was produced documenting the performance of the bridges under controlled live load tests (conducted during the summer in 2003 and 2005) and establishing the baseline response to environmental loads. At that time, the primary conclusions from the analyses were that all three bridge decks were behaving in a similar fashion and the differences in performance between the bridge decks were small. Preliminarily, the HPC deck was thought to potentially offer the most cost effective performance of the three deck configurations, followed closely by the Conventional deck, and more distantly by the Empirical deck. In 2009 a follow-on study was conducted to collect additional data to characterize the bridge decks and determine which configuration may offer the best performance.

Material tests and topographic surveys of the bridge decks done in 2009 revealed few differences between the decks and with results generally similar to the data collected in 2005 (the last time these tasks were done). The half-cell potential tests revealed little potential for corrosion, which is not surprising given the relatively young age of the decks and the sealant applied to the deck

surface shortly after construction. The topographic surveys showed minor differential settlements in the longitudinal direction of less than 5 mm.

Visual distress surveys revealed various types of cracking distresses, mostly concentrated near the abutments. A comparison between the three decks generally indicated that cracking near the abutments and over the bents was most pronounced in the Conventional and Empirical decks, and that these distresses were very similar between these two decks. While the HPC deck did not exhibit as much cracking near the abutments, the HPC and Conventional decks had a greater number of hairline cracks on the underside of the deck when compared to the Empirical deck. From the visual distress data collected thus far, it appears that: 1) the HPC deck is performing somewhat better than the other two decks, and 2) the Conventional and Empirical decks are performing very similar to one another. It is anticipated that these differences will become more apparent as the bridge decks mature.

Total strains at several locations within each deck were compared between the different bridges. In general, the decks are all responding similarly, where this response consists of temperature related diurnal strain cycles superimposed on temperature related seasonal strain cycles, all of which are superimposed on long term shrinkage strains. Statistical comparisons between the bridges revealed some differences between long term strains in both the transverse and longitudinal directions.

In the transverse direction, the magnitude of the mean strain in the HPC deck, consisting of a contraction (shrinkage) of about 320 microstrain, was less than in the Conventional and Empirical decks, which consisted of a contraction of about 380 microstrain. This is not surprising as the shrinkage strains measured in concrete samples collected during deck construction revealed lower shrinkage strains in the HPC deck concrete. The rates of change in the long term transverse strains within each bridge deck over time were very similar; had differences in these rates been discovered, they may have offered an indication of more (or less) stability in deck behavior and correspondingly reflected a possible increase (or decrease) in projected relative deck life. In the longitudinal direction, the bridge decks experienced similar strain levels in areas away from the bents and abutments. The differences between the bridges observed near the abutments appear to be heavily influenced by behaviors associated with localized behaviors of the integral abutments.

Overall the bridge decks appear to be performing well. Based on all the information obtained to date, the HPC deck will potentially offer the most cost effective performance of the three deck configurations. This conclusion is primarily based on the relative visual distresses observed in the decks and the lower magnitude strains generally seen in the HPC deck. Nonetheless, this conclusion must still be considered “preliminary” until it can be confirmed (or refuted) based on additional study of the decks’ performance over time.

TABLE OF CONTENTS

LIST OF FIGURES

LIST OF TABLES

1 INTRODUCTION

In 2003, the Montana Department of Transportation (MDT) replaced three bridges on Montana Secondary Highway 243 less than a mile north of Saco, Montana. The three bridges are within one mile of each other and are identical in geometry and design with the exception of the decks. A different deck design was purposefully used in each bridge in an effort to determine if any one design offered superior performance and cost-effectiveness based on their relative performance over time. The "Conventional" bridge deck (used as a control in this experiment) was designed using the standard practices of MDT's Bridge Bureau, and utilized a conventional concrete and standard reinforcement layout. The "Empirical" bridge deck was designed using the empirical design approach specified by the American Association of State Highway and Transportation Officials (AASHTO) Load & Resistance Factor Design (LRFD) Specification for Highway Bridges, which allows for a significant reduction in the steel reinforcement in conjunction with the standard deck concrete (AASHTO, 2000). The high performance concrete ("HPC") bridge deck was designed with a standard reinforcement layout (as in the Conventional deck), but a high performance concrete mix was used for the deck concrete.

For the first two years following their construction, the behavior of the bridge decks was intensively monitored by the Western Transportation Institute (WTI) in an effort to identify any early differences in their performance (Phase I study). Monitoring consisted of a) measuring deck strains during live load tests to identify basic structural behaviors, b) measuring long term deck strains and temperatures to observe thermal, shrinkage, and settlement behaviors, c) documenting any visual distresses (i.e., cracking and spalling) over time, and d) measuring half-cell potentials to determine any evidence of rebar corrosion. After extensive analysis of all the data that was collected, it was concluded that the decks were generally performing structurally as anticipated, with only small differences in their relative behavior and condition (see Cuelho et al., 2006). This result was not necessarily unexpected, as the decks were relatively young at the time this work was done (the study period covered from their construction through the second year they were in service). A follow-on evaluation of the bridge decks (Phase II study) was initiated after they had been in service for seven years to determine if more apparent differences were evident between them, and this evaluation is the subject of this report.

The objective of this project was to determine which of the three deck configurations may offer the best performance based on their relative behavior and physical condition now that they are seven years old. This objective was pursued by augmenting the extensive data collected earlier on these decks (i.e., from 2003 to 2008) with data collected in 2009, and then analyzing this data for indications of comparative differences in deck performance. The data collected in 2009 consisted of a subset of the data collected in the earlier study and included visual assessments of deck condition, electrical half-cell potential test results, and strains measured at selected locations in the decks under ambient conditions.

2 DESCRIPTION OF THE BRIDGES

The three replacement bridges were constructed on Montana Secondary Highway 243 approximately one mile north of Saco, Montana. Secondary 243 functions as a major collector and has an average daily traffic count of 320 (2008), with 8% being trucks. Much of the anticipated loading will come from heavy farm machinery and trucks, which can impose high demands.

All three bridges are 44.5 meters long and 9.1 meters wide (146 feet long and 30 feet wide). The superstructure consists of three spans, as shown in Figure 1. The stringers that support the deck are standard, Type-I prestressed concrete I-beams spaced at 2.4 meters (7.9 feet) on center, as shown in Figure 2. The thickness of each deck is 210 mm (8.3 in.). Design specifications for the bridge decks required 31 MPa (4,500 psi) strength concrete.

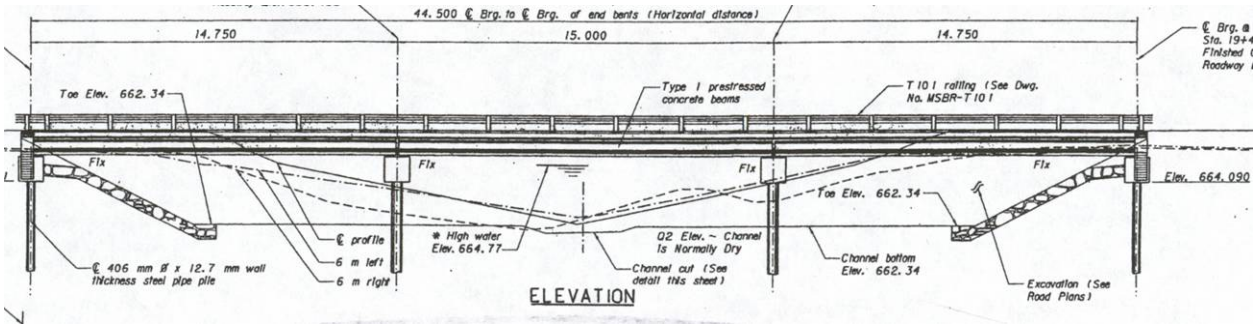

Figure 1: Elevation view of one of the bridges.

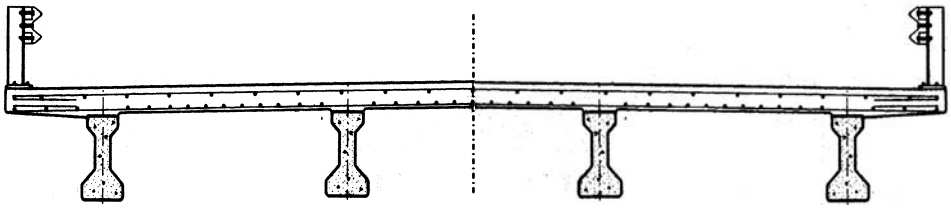

Figure 2: End view of Conventional bridge deck.

While all three decks use epoxy coated reinforcing steel, the layout of the reinforcing steel varies between the three decks. The conventional and HPC decks were designed using the traditional strength approach described in the AASHTO specifications (AASHTO, 2000). The traditional strength design method treats the deck as if it were a beam in flexure spanning the stringers. This design results in the primary reinforcement oriented transversely to the span of the bridge.

The empirical design approach, which requires no formal analysis, is permitted by the AASHTO specifications for monolithic concrete bridge decks that satisfy specific conditions. Using this design method, reinforcement ratios for the top and bottom mat in both the longitudinal and transverse directions are simply functions of the depth of concrete and length of span. AASHTO specifies a minimum reinforcement ratio equal to 3.8 cm^2/meter (0.18 $in.^2$/ft) in each direction in

the top mat, and 5.7 cm^2/meter (0.27 $in.^2$/ft) in each direction in the bottom mat. The reason for the increased amount of steel in the bottom mat is for better crack control in the positive bending regions of the slab. Comparatively, in the construction drawings for the decks constructed as part of this research project, the Conventional and HPC decks require 3667 kg (8084 lb) more steel than the empirical deck (a 31 percent increase). Figure 3 shows the difference in the density of the reinforcement between the two deck designs, taken at the same place in the deck. Reducing the amount of steel in the empirical deck, especially in the top layer, decreases the opportunity for, and the affects of reinforcement deterioration.

Figure 3: Typical reinforcement densities of the Conventional and HPC Decks (left), and the Empirical Deck (right).

Epoxy-coated, Grade 60 steel rebar was specified for each of the bridge decks. The average yield strength was 478.5 MPa (66.4 ksi), the average tensile strength was 740.1 MPa (107.3 ksi) and the elongation at failure was 14.5%. Tests to evaluate the epoxy coating yielded acceptable results.

The concrete mix designs used by the Montana Department of Transportation for each of the bridge decks are detailed in Table 1. A 19 mm (3/4 in.) minus aggregate mixture was used in these mix designs. The average 28-day concrete strengths and moduli of elasticity determined from samples collected by WTI during the deck pours are shown in Table 2.

Table 1: Mix Designs for Deck Concrete

Components	Concrete Batch Quantities	
	Conventional and Empirical Decks	**HPC Deck**
Cement	366 kg/m^3	366 kg/m^3
Silica Fume (Rheomac SF100)	---	22.3 kg/m^3
Water	151.1 kg/m^3	129 kg/m^3
Coarse Aggregate (#4 – ¾")	1061 kg/m^3	1094 kg/m^3
Fine Aggregate (sand)	719 kg/m^3	693 kg/m^3
Air Entraining Solution	127 ml	325 ml
Water Reducing Agent	910.9 ml	911 ml
Superplasticizer	---	1455 ml
Properties		
Final Slump	40 – 80 mm	100 – 200 mm
Air Content	6% ± 1%	5 – 7%
Minimum 28-Day Strength	31 MPa	31 MPa

Table 2: Average 28-Day Compressive Strength and Modulus of Elasticity of the Concrete

Bridge	Strength (MPa)	Modulus of Elasticity (GPa)
Conventional	28.0	29.3
Empirical	27.4	27.8
HPC	46.0	31.5

Type I prestressed concrete beams were used to support the bridge deck. The dimensions and sectional properties of these beams are shown in Figure 4. The results of the concrete compressive strength tests for the prestressed girders (obtained from MDT) were averaged and are summarized in Table 3.

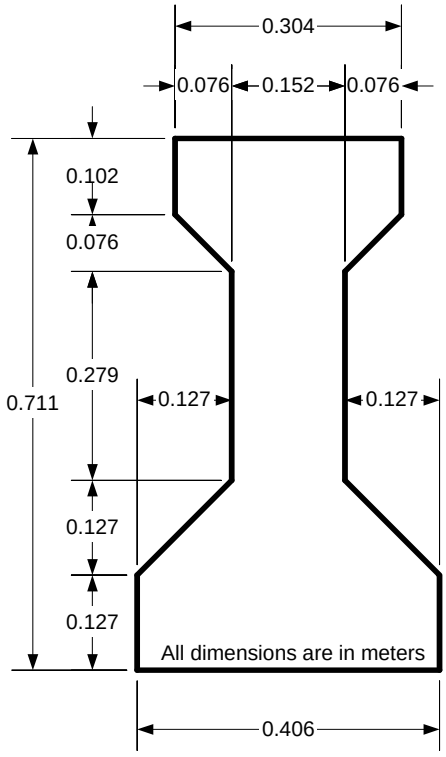

Figure 4: Dimensioned cross-sectional view of bridge girders.

Table 3: Average 28-day Prestressed Girder Concrete Compressive Strengths

Bridge	Strength (MPa)
Conventional	63.0
Empirical	61.0
HPC	64.2

3 MATERIAL TESTING AND VISUAL DISTRESS SURVEYS

Long term monitoring of the bridge decks consisted of assessing corrosion potential, mapping cracks, and measuring global movement of the bridge structures using survey equipment. The material testing and distress and topographic surveys provided important information about the changes in the physical condition of the bridge decks over time. The corrosion tests, measurements of concrete shrinkage, topographical surveys, and visual distress surveys were performed in 2003, 2004, and 2005 for the initial study and in 2009 for this follow-on study. Attempts were made to correlate behavior identified from the internal strain measurements to information obtained from these various surveys.

3.1 Corrosion Testing

Half-cell potential tests of concrete bridge decks can indicate the likelihood of corrosion activity within the reinforcing steel at the time of measurement. Because epoxy-coated reinforcing bars were used in the decks, copper lead wires were installed on two transverse and two longitudinal bars at the time of construction to allow half-cell potential measurements on these bars. Tests conducted in July 2003, 2004, and 2005 and August 2009 generally showed little indication of possible corrosion activity. In 2003 there were several locations that indicated some probability of corrosion occurring, but this was likely due to the chemistry of the pore water in the young concrete. By 2005, and still in 2009, all of the measurements indicated a 90 percent probability of no corrosion.

3.2 Concrete Shrinkage

Shrinkage of the concrete was monitored using small beam specimens cast during each deck pour. Some of the shrinkage beams were cured in a moist environment while the remainder were cured and stored on site. Shrinkage is highly dependent upon humidity; therefore, the shrinkage beams cured and stored with the bridge decks should most closely represent true shrinkage of the deck concrete. A milling machine equipped with an edge finder was used to precisely measure the lengths of the shrinkage beams periodically over the seven year interval since the bridge decks were cast. The resulting shrinkage strains (calculated as change in length divided by original length) are presented in Figure 5. Reported values are the mean values for measurements made on three shrinkage beams from each bridge deck.

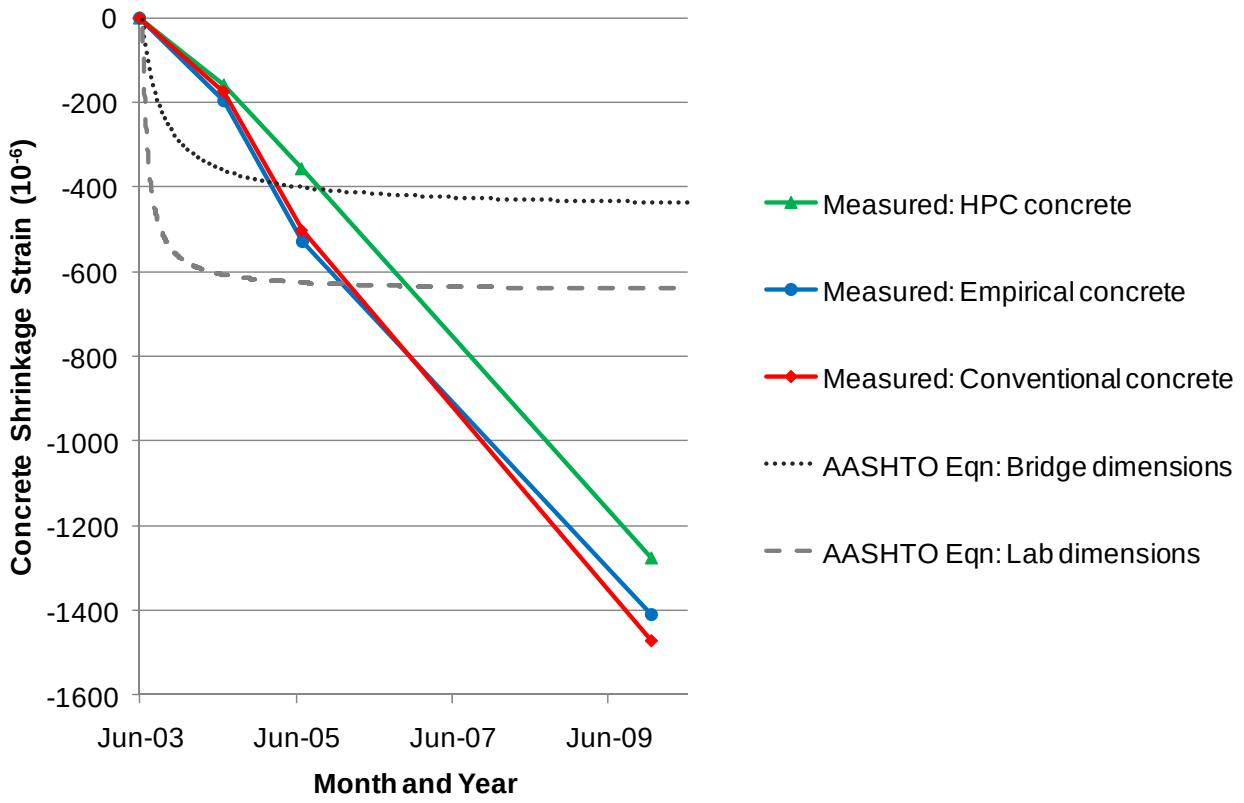

Figure 5: Concrete shrinkage of laboratory specimens compared to the AASHTO equation.

Referring to Figure 5, the shrinkage strains in the deck concretes have steadily increased since the specimens were cast during deck construction in 2003, reaching 1200 to 1400 microstrain in 2009. This result is unexpected, as typically the majority of concrete shrinkage occurs within the first year after construction, with long term values eventually reaching between 200 and 800 microstrain (ACI, 2008). Thus, both the nature and magnitude of the shrinkage strains measured in 2009 are unusual, with the cause for these unusual behaviors being uncertain. These measurements are exceptionally sensitive to the specific operator and equipment used, both of which changed between 2005 and 2009. That being said, the shrinkage of the HPC deck concrete has been noticeably less than that of the Conventional and Empirical deck concretes since 2005, by approximately 150 microstrain. Shrinkage in concrete is influenced by a myriad of factors, and thus it can be difficult to make a general statement about the relative shrinkage of high performance compared to traditional concretes. In this case, the specific concrete used in the HPC deck had a lower absolute volume of water in the mixture than was used for the Conventional and Empirical deck concretes (refer to Table 1), and thus it would be expected to exhibit less shrinkage than those concretes (Zia et al., 1997).

To provide further perspective on shrinkage of the deck concrete, the expected shrinkage was also calculated using an equation available for this purpose in the AASHTO bridge design specifications (Equation 1 below). Estimated shrinkage as a function of time calculated using

these values is also shown in Figure 5. Note that a single curve describes the expected shrinkage behavior of all three bridge decks, as the cited AASHTO equation does not include variables that address differences in the deck concrete.

$$\varepsilon_{Sh} = -k_s \cdot k_h \left(\frac{t}{35 + t} \right) \cdot 510 \qquad \textbf{Equation 1}$$

where

$$k_s = \left(\frac{\frac{t}{26 \cdot e^{0.36 \cdot V/S} + t}}{\frac{t}{45 + t}} \right) \left(\frac{1096 - 94 \cdot V/S}{923} \right)$$

$$k_h = \frac{140 - H}{70}, \text{ for } H < 80\%$$

$$k_h = \frac{3 \cdot (100 - H)}{70}, \text{ for } H \geq 80\%$$

ε_{Sh} = shrinkage microstrain ($\mu\varepsilon$)

H = average annual relative humidity (%)

t = time since the concrete was removed from curing (days)

V/S = volume to surface area ratio (inches) $\{1.0 \leq V/S \leq 6.0\}$

Based on the AASHTO concrete shrinkage model, the concrete bridge decks have experienced approximately -430 $\mu\varepsilon$ through June 2010. As shown in Figure 5, the measured shrinkage was significantly larger than the calculated shrinkage. One likely explanation for this is that "large concrete members may undergo substantially less shrinkage than that measured by laboratory testing of smaller specimens of the same concrete" (Russell et al., 2006). This is primarily attributed to the effects of reinforcement and other bridge elements, which were not present in the measured shrinkage specimens. When the equation is adjusted based on the dimensions of the shrinkage specimens, the estimated shrinkage is greater, but still less than the measured shrinkage (Figure 5).

3.3 Topographic Surveys

Topographic surveys were conducted to measure relative changes in the elevation and the horizontal position of various points on the surface of each deck. The same reference points were used in all surveys and are shown in Figure 6. Horizontal position was measured with an accuracy of about 3 mm and elevation was measured with an accuracy of approximately 1 mm.

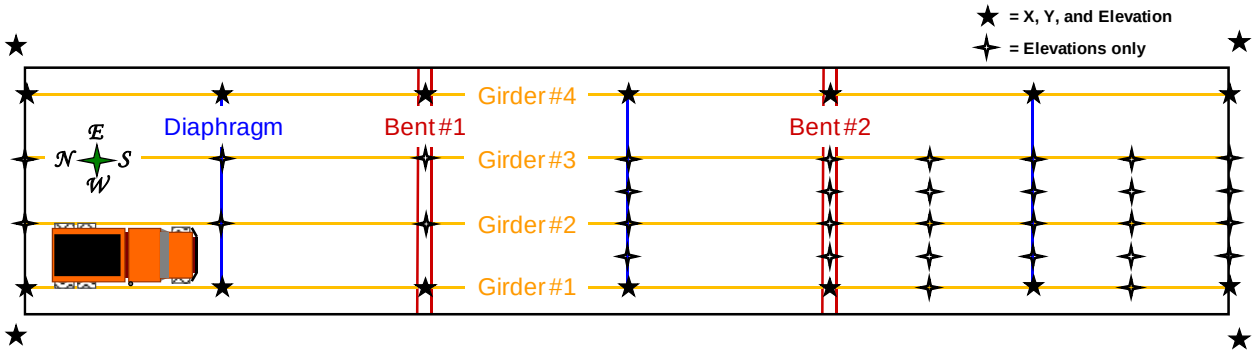

Figure 6: Survey points on a plan view of a bridge deck.

The results of the elevation surveys conducted in 2003, 2005, and 2009 are overlaid for each bridge in Figure 7, Figure 8 and Figure 9 for the Conventional, Empirical, and HPC decks, respectively. The geometry of the surfaces of all the decks was similar, consisting of a basic crown down the centerline of the bridges (measured as approximately 1.5 percent) and some longitudinal camber (upward deflection) between the bents, most notably in the HPC bridge. Elevation changes over time were small, although the survey conducted in 2009 showed some "tilting" of all the bridges along their longitudinal axis, with a small increase in elevation of approximately 0.5 mm (0.02 in.) on the north end, and a decrease of about 5 mm (0.2 in.) on the south end.

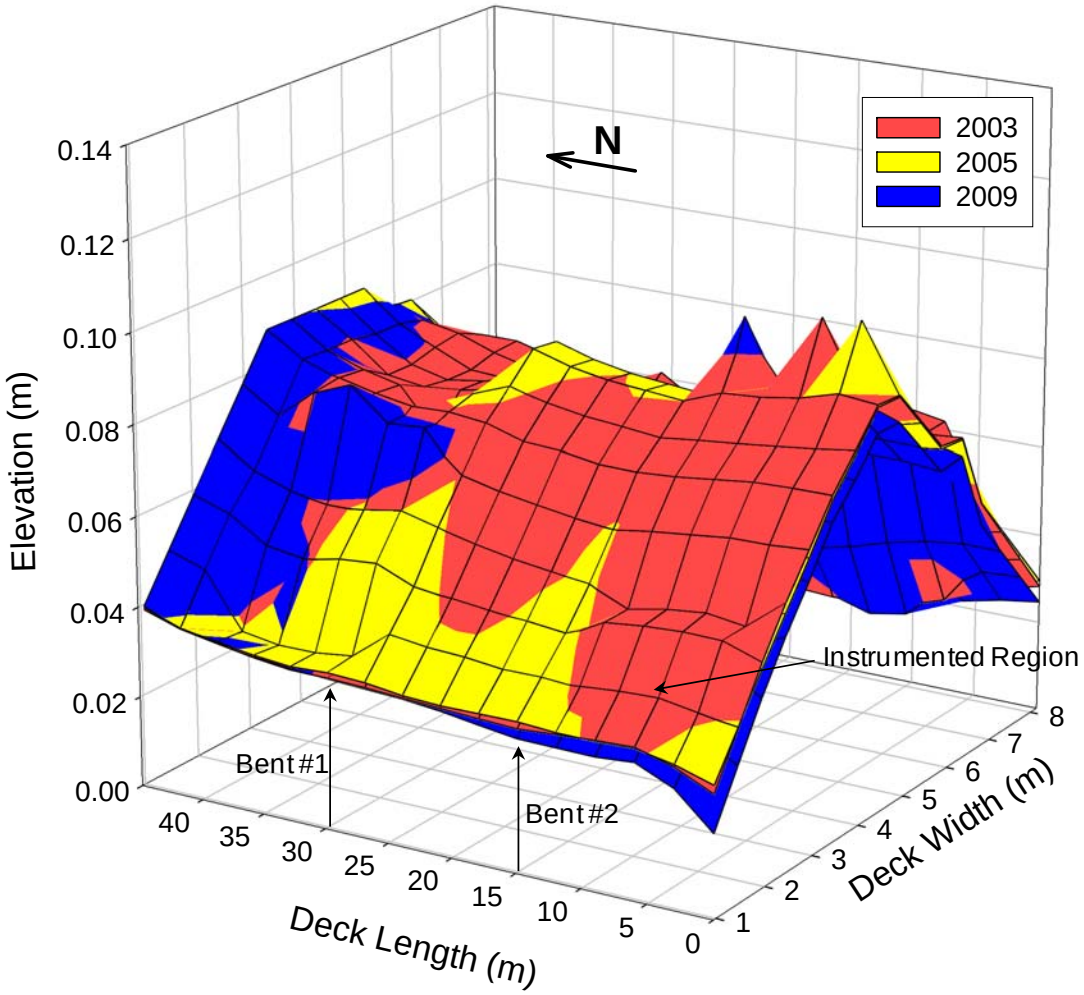

Figure 7: Topographic map of Conventional bridge deck surface.

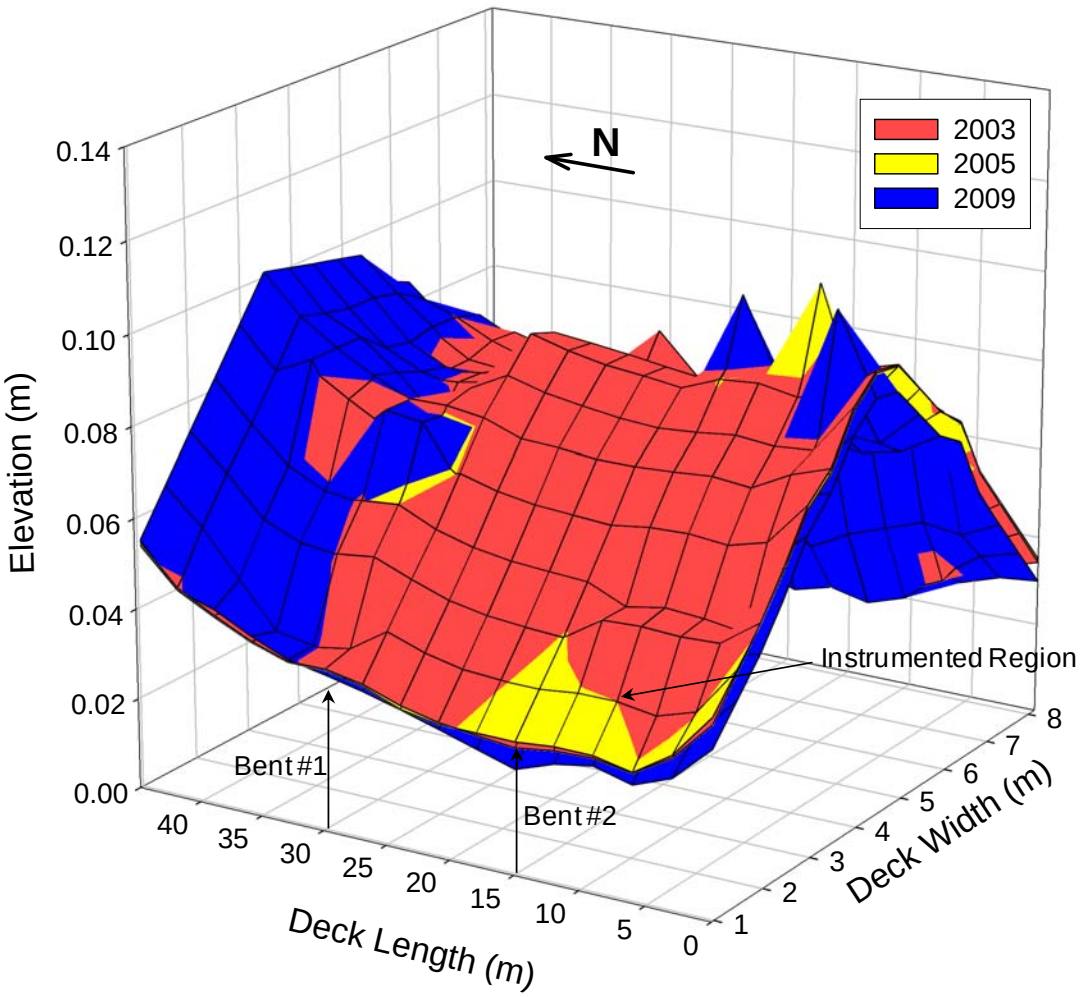

Figure 8: Topographic map of Empirical bridge deck surface.

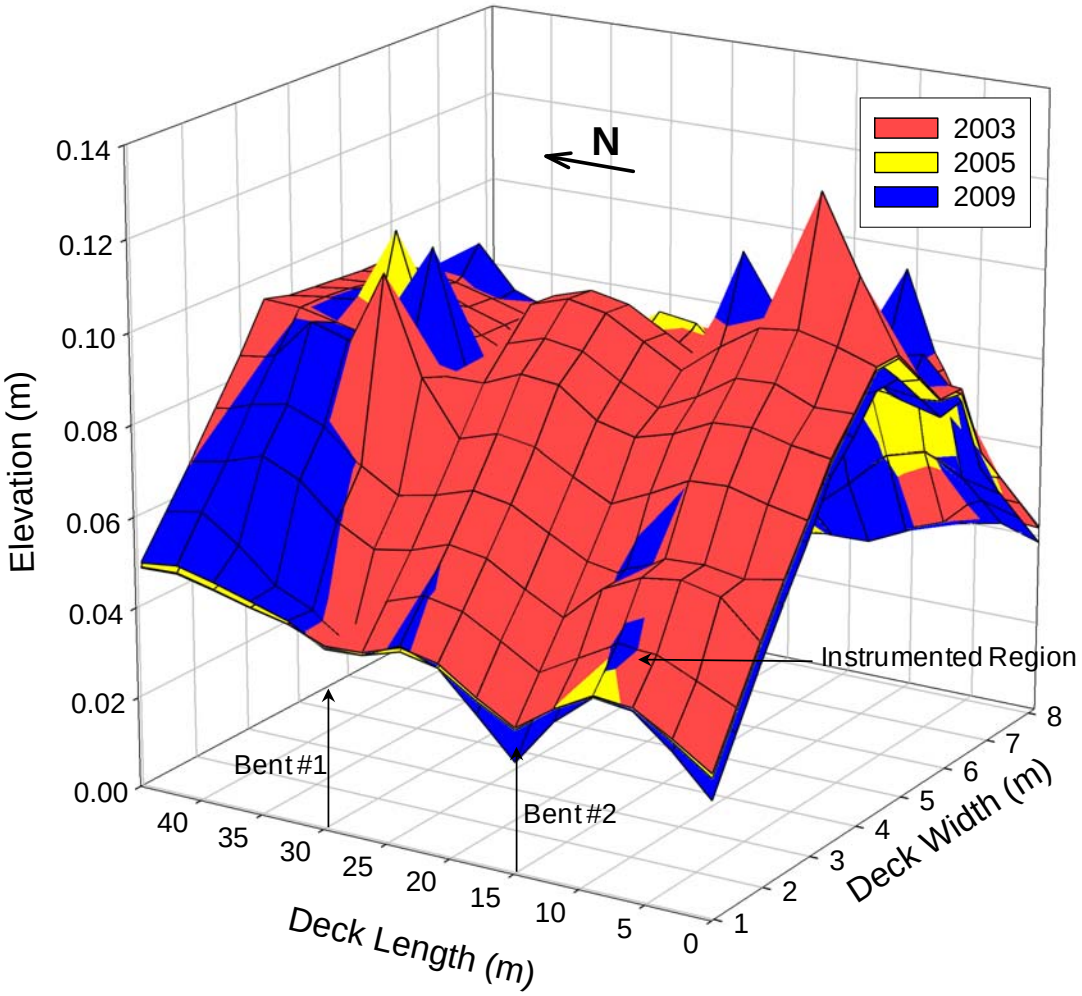

Figure 9: Topographic map of HPC bridge deck surface.

3.4 Visual Distress Surveys

The three bridge decks were closely inspected to monitor the development of cracks, irregularities and delaminations. Acoustical soundings using a chain drag revealed no delaminations in the deck surface. Visible cracks were highlighted with a black marker and photo-documented. Consistent with the Phase I surveys, the entire top surface of the deck was inspected, whereas only about one-third of each end span toward the abutments was examined on the underside. A comprehensive survey of the underside of the bridge decks was not possible without special equipment. Thus, only the portion of the underside readily accessible from below the bridges was examined. Crack maps were generated and compared with visual distresses in 2005 (the last time visual distresses were surveyed). The 2005 and 2009 distress surveys are shown in Figure 10 and Figure 11, respectively.

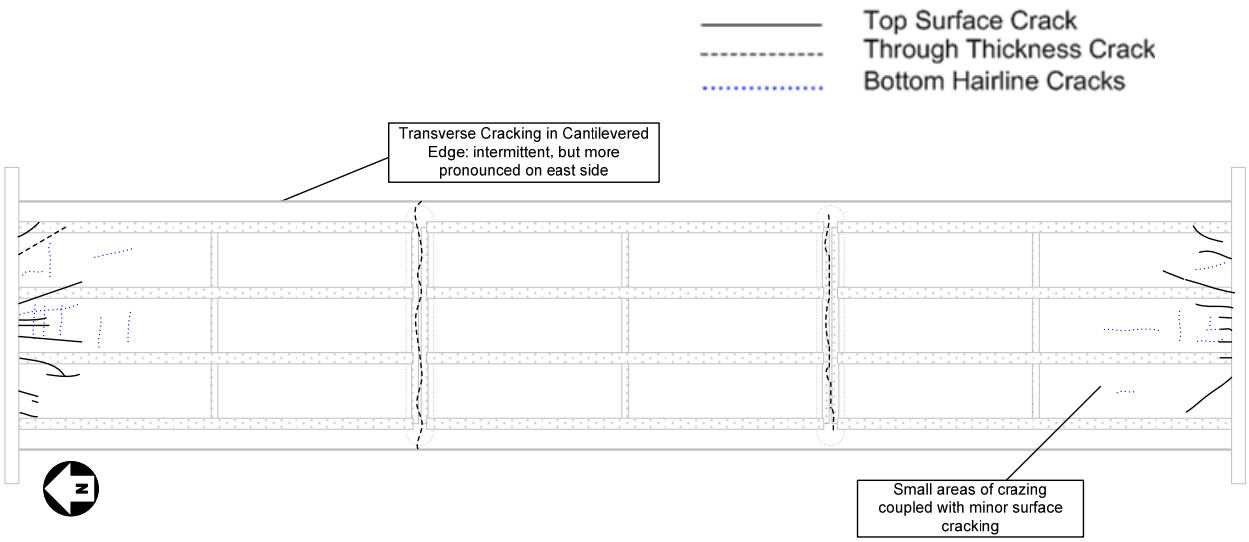

a) Conventional Bridge – 2005

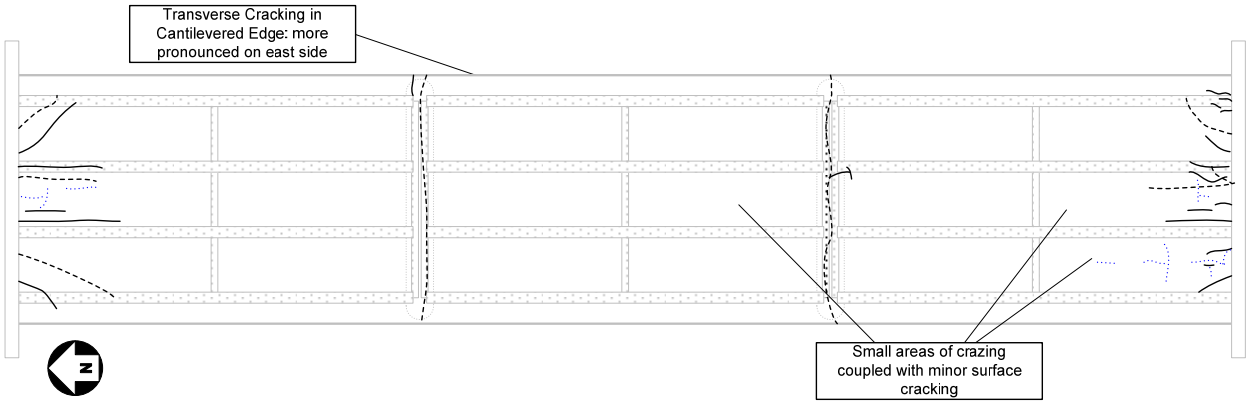

b) Empirical Bridge – 2005

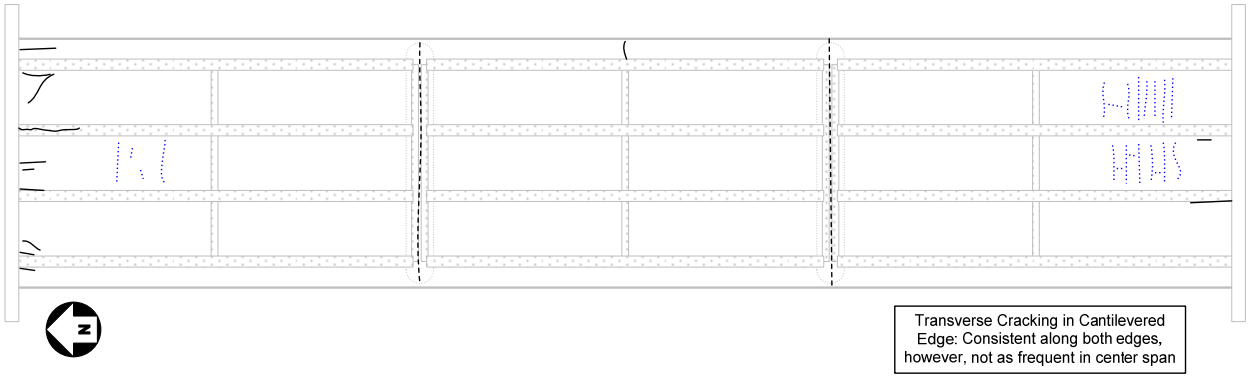

c) HPC Bridge – 2005

Figure 10: Visual distress survey maps of the Saco bridge decks – 2005.

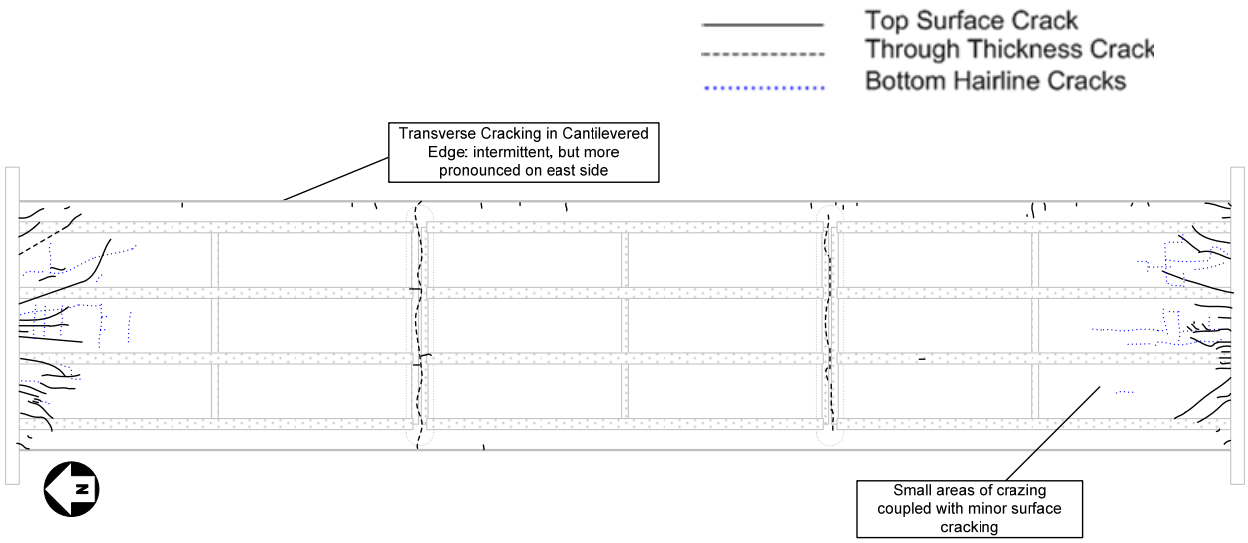

a) Conventional Bridge – 2009

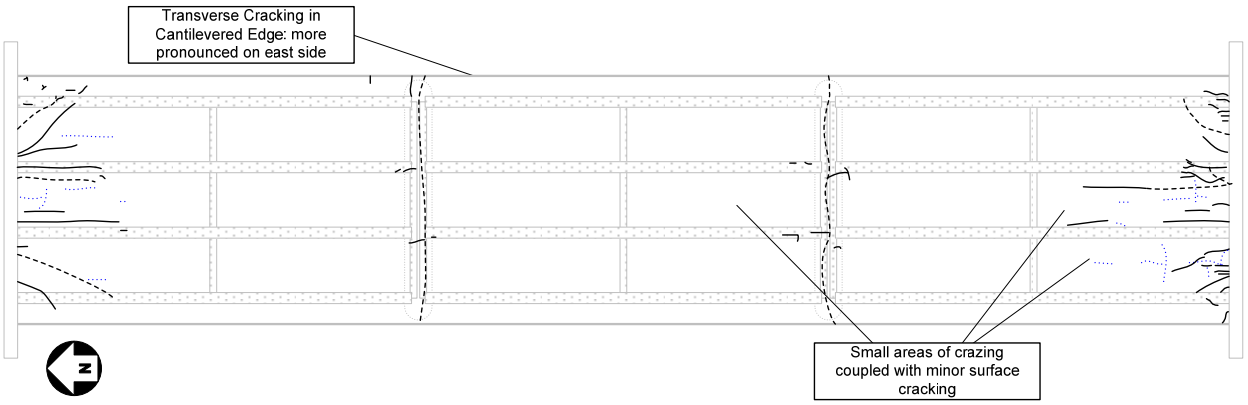

b) Empirical Bridge – 2009

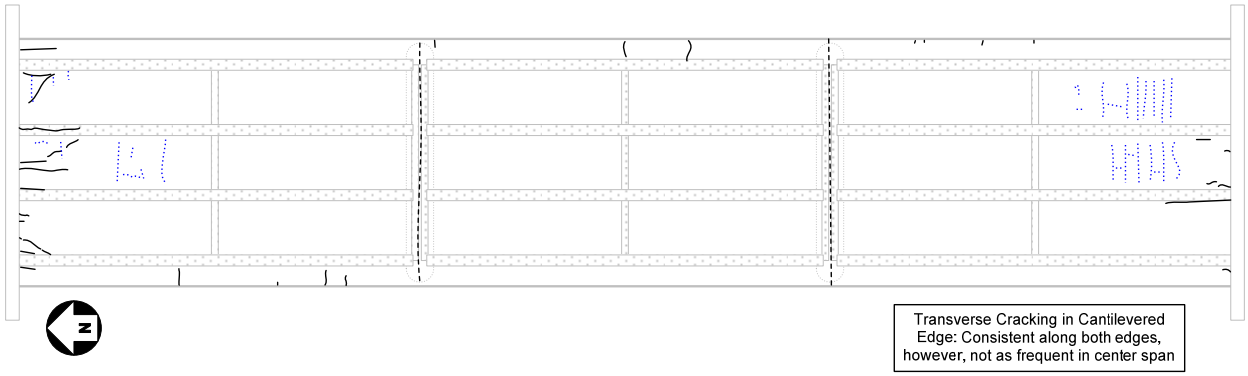

c) HPC Bridge – 2009

Figure 11: Visual distress survey maps of the Saco bridge decks – 2009.

3.4.1 Cracking over the Bents

Transverse cracks developed over each of the bents within days after the deck concrete was placed, as described during the Phase I study. Generally, these cracks had not changed dramatically in 2009, other than further cracks developing in the Conventional and Empirical decks in the longitudinal direction initiating at the transverse cracks. Some of this type of cracking was already evident on the Empirical deck in 2005, but by 2009 more cracks had formed over both bents (Figure 11). By 2009 the Conventional deck also exhibited some longitudinal cracks propagating from the northern (non-saw-cut) bent as shown in Figure 12. Overall, the longitudinal cracking coincident with the transverse cracking over the bents was most prominent in the Empirical deck, present in the Conventional deck, and was not found in the HPC deck.

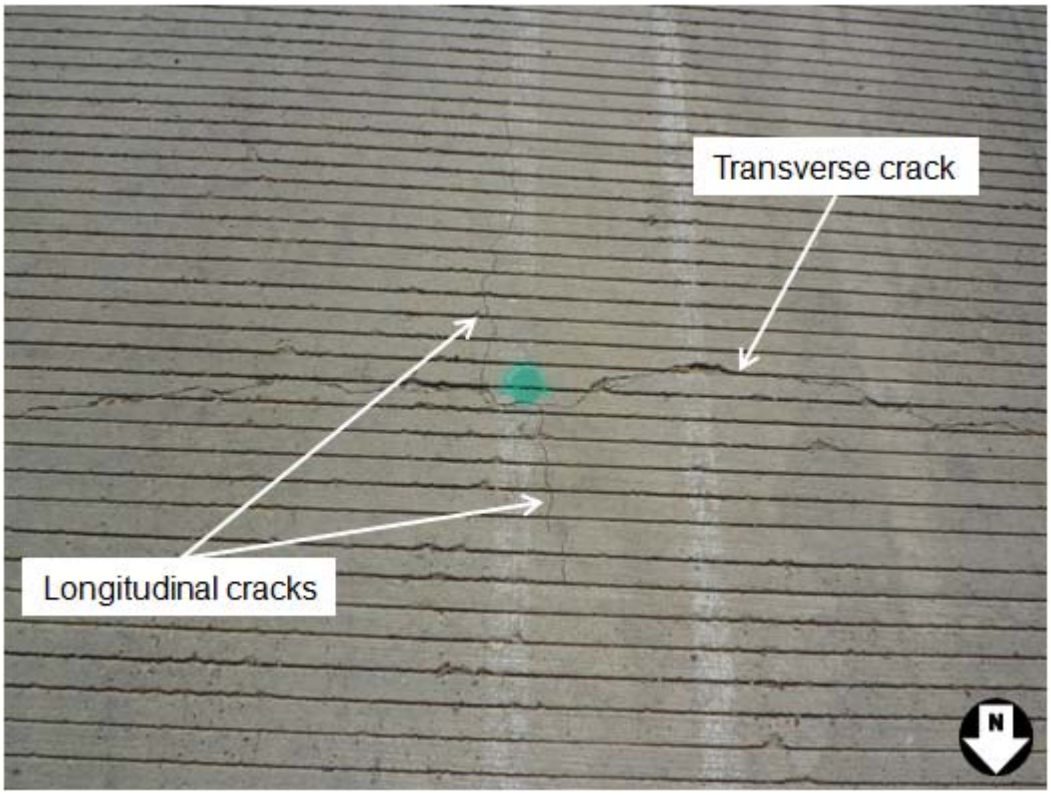

Figure 12: Longitudinal cracking propagating from the transverse crack over the northern bent of the Conventional deck.

3.4.2 Top-Surface and Full-Depth Cracking Near the Abutments

The majority of the cracking on all three bridge decks has occurred on the ends near the abutments. By 2005, fairly significant cracking was evident in this area, but was even more pronounced in 2009 with an increase in the number of cracks and length of existing cracks. The HPC deck still showed less cracking in these areas than the Conventional and Empirical decks. The southwest end of the Conventional and Empirical decks is shown in Figure 13 and Figure

14, respectively. Looking more specifically at the Conventional and Empirical decks, the following observations were made.

- The level of cracking distresses in the Conventional deck was more similar to the cracking distresses in the Empirical deck than during previous assessments.
- The Empirical deck had more full-depth cracking near the abutments.
- On the north end, the Conventional deck had a larger number of cracks on the top surface of the deck, but they were generally shorter than the cracks in the Empirical deck.

Figure 13: Cracking on the southwest end of the Conventional deck in 2009.

Figure 14: Cracking on the southwest end of the Empirical deck in 2009.

3.4.3 Full-Depth Transverse Cracking Near the Cantilevered Edges

The cantilevered edges of all the decks exhibited short full-depth transverse cracks. This cracking was first noticed on the HPC deck in 2004, but by the end of Phase I each bridge exhibited some cracking in this area. The Conventional and Empirical decks had more cracking on the east edge, while the HPC deck had similar cracking on both edges. As shown in Figure 11 and Figure 15, the cracks were generally longer in the HPC deck, but more numerous in the Conventional deck. The cantilevered edge cracking was least severe in the Empirical deck.

Figure 15: Cantilever edge cracking, eastern edge, HPC–left, Conventional–right, in 2009.

3.4.4 Hairline Cracking on the Underside of the Deck

In areas on the underside of the decks readily accessible for inspection (i.e., near the abutments), longitudinal and transverse hairline cracking was observed between the girders. In 2005 the cracking was most severe in the HPC deck. This cracking was relatively unchanged between 2005 and 2009 in the HPC deck, while over this same period this cracking increased in the southern end of the Conventional deck, and is similar in extent to the HPC deck. The Empirical deck still exhibits the least severe cracking in this area.

3.5 Bridge Approaches

Settlement of the bridge approaches was qualitatively assessed in 2005 by placing a straight edge along the bridge deck with one end cantilevered over the paved approach. Northbound traffic approaches the bridge decks on the southeast (SE) end; likewise, southbound traffic approaches the bridge decks on the northwest (NW) end of the bridge. Pictures taken from the side allowed a qualitative comparison of the settlement that has occurred in the paved approaches. The same procedure was used in Phase II (Figure 16 to Figure 18), although in addition to photographs, measurements of the gap between the straight edge and the pavement were recorded. For northbound traffic, the gap is largest in the HPC deck (2 cm), followed by the Empirical deck (1.5 cm), and finally the Conventional deck (1 cm). For southbound traffic, the gap is very similar for all the bridge decks (2–2.5 cm). This is notably different than the findings in 2005 in which the Empirical deck showed large settlements on this approach (Figure 19).

Figure 16: Paved approaches of the Conventional deck (NW-left, SE-right) in 2009.

Figure 17: Paved approaches of the Empirical deck (NW-left, SE-right) in 2009.

Figure 18: Paved approaches of the HPC deck (NW-left, SE-right) in 2009.

Figure 19: Paved approaches of the Empirical deck (NW) in 2005 (left) and 2009 (right).

3.6 Summary

Deterioration of bridge decks is influenced by a complex combination of numerous factors initially related to design, materials and construction and subsequently affected by external

factors such as temperature, traffic loading, and differential settlement of the structure. Corrosion testing, visual distress monitoring and topographic surveying of the Saco bridges were used to assess the condition of the decks. In general, each of the bridge decks showed very little potential for corrosion based on the half-cell tests. This result is not surprising given the relatively young age of these structures. Other than some nominal longitudinal tilting of the structures, differential movements of the decks was relatively small (on the order of 1 to 5 mm across the length of the deck), based on the topographic surveys. The approaches to the bridges were also similar to one another, and thus would not be expected to be responsible for generating any significant differences in the deck responses between the structures.

Visual distress surveys revealed various types of cracking distresses, mostly concentrated near the abutments. A comparison between the three decks generally indicated that cracking near the abutments and over the bents was most pronounced in the Conventional and Empirical decks, and that these distresses were very similar between these two decks. While the HPC deck had not exhibited as much cracking near the abutments, the HPC and Conventional decks had a greater number of hairline cracks on the underside of the deck when compared to the Empirical deck. From the visual distress data collected thus far, it appears that: 1) the HPC deck is performing somewhat better than the other two decks, and 2) the Conventional and Empirical decks are performing very similar to one another. It is anticipated that these differences will become more apparent as the bridge decks mature.

4 DESCRIPTION OF THE EMBEDDED INSTRUMENTATION

During construction, the bridge decks were instrumented with a suite of sensors to monitor the strain and temperature at several locations generally concentrated on the southwest end of the bridges. Long term strain monitoring was accomplished using vibrating wire gages embedded in the concrete which generally maintain greater stability and survivability over time than electrical resistance strain gages. The longitudinal and transverse vibrating wire gages were installed at the time the decks were constructed in the locations shown in Figure 20.

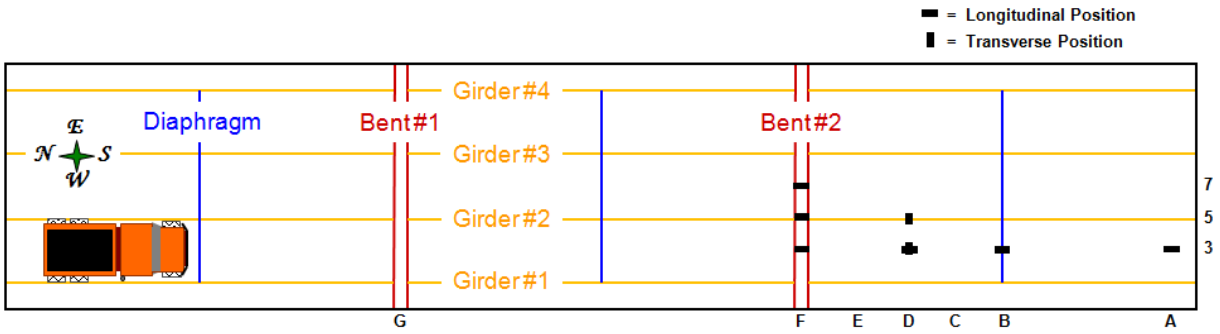

Figure 20: General location of vibrating wire gages (plan view).

Referring to Figure 20, Gage line F was instrumented to assess bending across the bent as well as the bent–stringer interaction. Position D-3 was instrumented to study local deck behavior—it is located equidistant between two stringers and the bent and diaphragm. Position D-5 was instrumented to study behavior immediately over an interior stringer. Position B-3 was instrumented to investigate deck response midway between the bent and the abutment between two stringers. Finally, position A-3 was instrumented to assess the effects of the abutment on the bridge deck. Note that the decision was made in Phase I of this effort to focus on "typical" deck behaviors as opposed to abutment-specific behaviors; thus only two gages were installed in this area and only in the longitudinal direction.

The vibrating wire strain gages (Model VCE-4200) were purchased from Geokon (Lebanon, New Hampshire). This standard model, shown in Figure 21, has a 153 mm (6.0 in.) gage length, 3000 με range, and 1 με sensitivity. They are designed to be embedded directly in concrete and are typically used to monitor long-term strain and temperature in structures such as foundations, piles, bridges, dams, containment vessels, and tunnel liners.

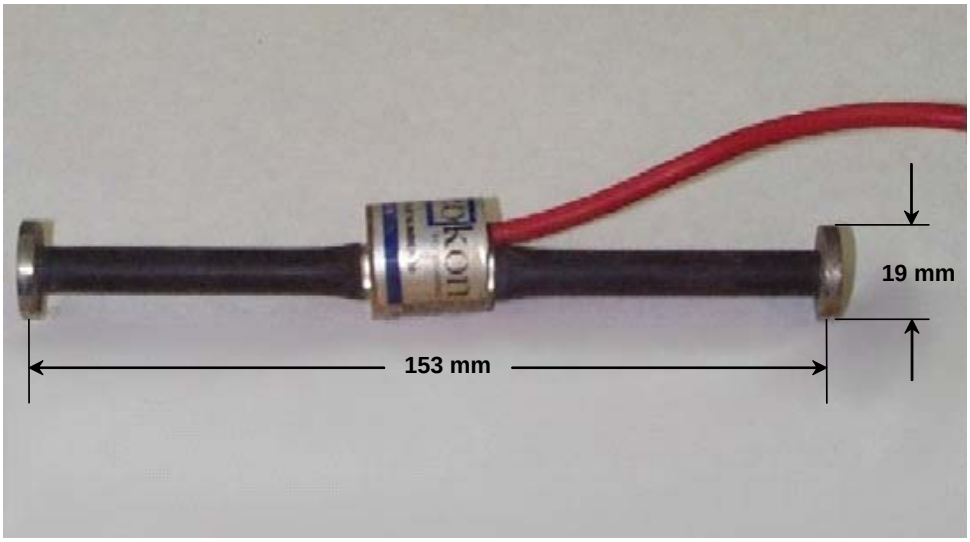

Figure 21: Vibrating wire strain gage.

The gages use a steel wire in tension between two circular end plates to measure length changes in the concrete. As the concrete contracts or expands, the wire responds accordingly, thereby changing its resonant frequency of vibration. The wires are excited by electromagnetic coils, which also detect their resonant frequencies of vibration. Frequencies detected by the coil are converted to a DC voltage using a vibrating wire interface unit. Each vibrating wire gage is also equipped with a thermistor to record temperature. Temperature measurements are used to apply temperature corrections to measured strains, necessitated by differences between the thermal expansion coefficients of steel and concrete.

A reference numbering system was created to help organize and distinguish each gage based on its location, orientation, type, and relative position. Altogether, the gage numbering system consists of six characters, as illustrated in Figure 22. The global location indicates which bridge the sensor is embedded in: Conventional (C), Empirical (E), or HPC (H). Gages are oriented either longitudinally (L) or transversely (T) with respect to the direction of traffic. Gage types are either strain gages bonded to the reinforcement (R), vibrating wire gages (V), or embedded concrete gages (E). The analysis in this follow-on study focused on the vibrating wire sensors. Positions of the gages are referenced from the southwest corner of the bridge. Longitudinal distances from the south end of the bridge are denoted by the letters A through G. Transverse positions of the gages from the west side of the bridge are denoted by the numbers 1 through 7 (these correspond to the letters and numbers in Figure 20). Finally, the vertical position of each gage within the deck is described as bottom (B), middle (M), or top (T). The example in Figure 22 (C-LV-F-3-B) corresponds to a **L**ongitudinally oriented **V**ibrating wire gage in the **C**onventional bridge deck, located at Gage Line **F**, transverse position **3**, and in the plane of the **B**ottom mat of reinforcement. These unique reference numbers are used throughout the remainder of the report.

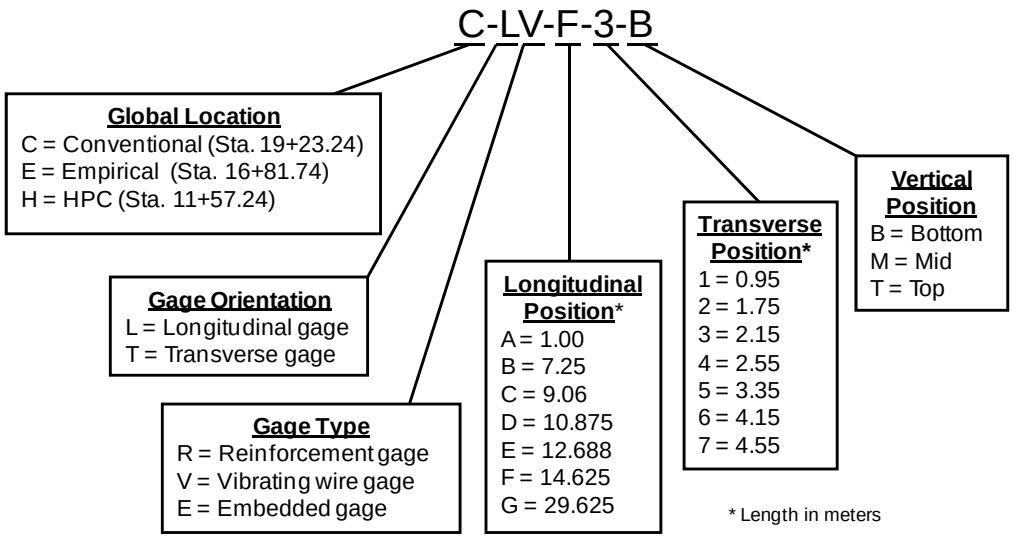

Figure 22: Gage reference numbering system.

At the end of Phase I an assessment of gage survivability showed almost 50 percent of the electrical resistance strain gages (attached to reinforcement or embedded in concrete) had failed by summer 2005. During this same time period, vibrating wire gage survivability was significantly greater with only three failed gages in each of the Conventional and Empirical decks and none in the HPC deck. By fall 2009 almost 70 percent of the electrical resistance strain gages were not working properly, while only 22 percent of the vibrating wire gages had failed (Table 4). Overall, while the vibrating wire gages demonstrated better survivability than the bonded and embedded electrical resistance gages, half of the vibrating wire gages in the Conventional deck did not work properly when assessed in 2009. Appendix A contains a complete list of the gage failures over time.

Table 4: Cumulative Number and Percent of Gage Failures as of Fall 2009

Cumulative Gage Failures (Number)				
Bridge Deck	**Resistance**	**Embedded**	**Vibrating Wire**	**All Gages**
CON	25	6	10	41
EMP	20	4	3	27
HPC	29	7	0	36
All Decks	74	17	13	104

Cumulative Gage Failures (Percent)				
Bridge Deck	**Resistance**	**Embedded**	**Vibrating Wire**	**All Gages**
CON	71%	17%	50%	21%
EMP	57%	11%	15%	14%
HPC	83%	20%	0%	19%
All Decks	70%	63%	22%	54%

A solar-powered data acquisition system was located at each bridge consisting of a Campbell Scientific CR5000 datalogger, two multiplexers, a vibrating wire interface, and Wheatstone bridge circuits. The system accommodated 42 resistance strain gages and 16 vibrating wire strain gages, although only the vibrating wire gages were used in this evaluation. At the top of each hour the CR5000 was activated and measured the strain and temperature of all the gages. A more detailed explanation of the instrumentation plan is provided in Cuelho et al. (2006).

5 RESULTS AND ANALYSIS OF LONG-TERM STRAIN DATA

The primary goal of this project is to compare the relative performance of the three bridge decks. As part of this process, the long-term strain data can be used to develop an understanding of how each bridge deck has responded to seasonal temperature fluctuations, shrinkage of the concrete and creep—the primary agents by which these decks have matured during the past seven years.

Both qualitative and quantitative observations and comparisons of the available strain data are presented, as possible and appropriate. While qualitative assessments are valuable in generally describing differences in performance between the three bridge decks, they are of limited use unless these differences are pronounced in nature. That is, subtle differences in behavior may be impossible to detect simply by qualitative observation. Indeed the important, qualitatively based conclusion that can be readily drawn after reviewing the long-term strain data is that all three decks are behaving in a similar fashion. The decks, however, are not behaving identically. Thus the issue becomes whether or not consistent patterns exist in the small variations in the long-term response between the decks that reflect true differences in behavior. This question can possibly be answered through some form of quantitative analysis of the data. Statistical methods were employed to perform these quantitative comparisons, as described in more detail below.

Data collection began in summer 2003 when the bridge decks were constructed and continued until June 2008 with few interruptions. The Phase I analysis was based on data collected through June 2005 when the bridges were two years old. WTI continued to collect data from June 2005 to June 2008 beyond the analysis period of the original project. In June 2008 the data acquisition systems were disconnected (effectively, at the beginning of year six) until they were reinstalled in August 2009 and operated until May 7, 2010 for this follow-on project.

5.1 Data Treatment and Analysis Methods

At any instant in time, the total strains experienced by the bridge decks are the net combination of four effects: load, temperature, shrinkage and creep. Often, attention is focused on load related strains; however, the decision was made to investigate total strain, because the long term strains were expected to be dominated by temperature and shrinkage effects.

Output from each of the vibrating wire strain gages included load, shrinkage, and creep effects, but was automatically compensated for temperature effects. Therefore, the data had to be processed to restore the temperature contribution to the total strain. This processing consisted of modifying the recorded response by the difference between the coefficient of thermal expansion of the deck concrete and the reinforcing steel, multiplied by the change in temperature. Values of the coefficient of thermal expansion (CTE) of each deck concrete were required to make this adjustment. A laboratory experiment conducted during Phase I demonstrated that the CTEs for the concrete are temperature-dependent. A sixth-order polynomial for the CTE of concrete (Equation 2) developed during Phase I was used to more accurately characterize the thermal

strain in the bridge decks as a function of temperature (Johnson, 2005), where *T* is the temperature in Celsius. The values for thermal strain were corrected using Equation 2 as part of the data analysis.

$$CTE = -2.03271\times10^{-9}T^6 + 4.58388\times10^{-8}T^5 + 4.2392\times10^{-6}T^4 - 8.27969\times10^{-5}T^3 - 0.00171668T^2 + 0.08695897T + 9.8950516$$

Equation 2

where

T = temperature (°C)

Plots of long term total strain data from the beginning of Phase I of this project through the end of Phase II were created to qualitatively analyze general behaviors at each location in the deck. The bridge decks experience both diurnal and seasonal temperature cycles. The strain response in the concrete to these frequent temperature cycles was evident in the data and to a certain extent interfered with formulating comparisons of the average values and seasonal fluctuations in the strain response between bridges (see insert in Figure 23). In order to more easily observe differences between the bridge decks, the strain data was smoothed using a 1-week moving average, as was done in the Phase I investigation. A representative example of this smoothed data is shown in Figure 23, and Appendix B contains plots of the smoothed strain response for all gages that were monitored. In general, plots of strain over time along the A-, B- and D-lines were similar to one another; nevertheless, small changes over time were also observed as detailed below. The long-term strain levels along the F-line, however, were less similar to one another, as illustrated by the strain response at position F-3-B, where the strains differed from one another at a given point in time and continued to diverge over time (Figure 24). Strain responses along the F-line were known to be heavily influenced by local behaviors of the transverse cracks that developed in this region. The ability of the instrumentation along the F-line to reflect the development of such distresses was substantiated during phase I by showing 1) a shift in the absolute magnitude of strain, and 2) the increase in diurnal temperature related strain fluctuation (Cuelho et al., 2006).

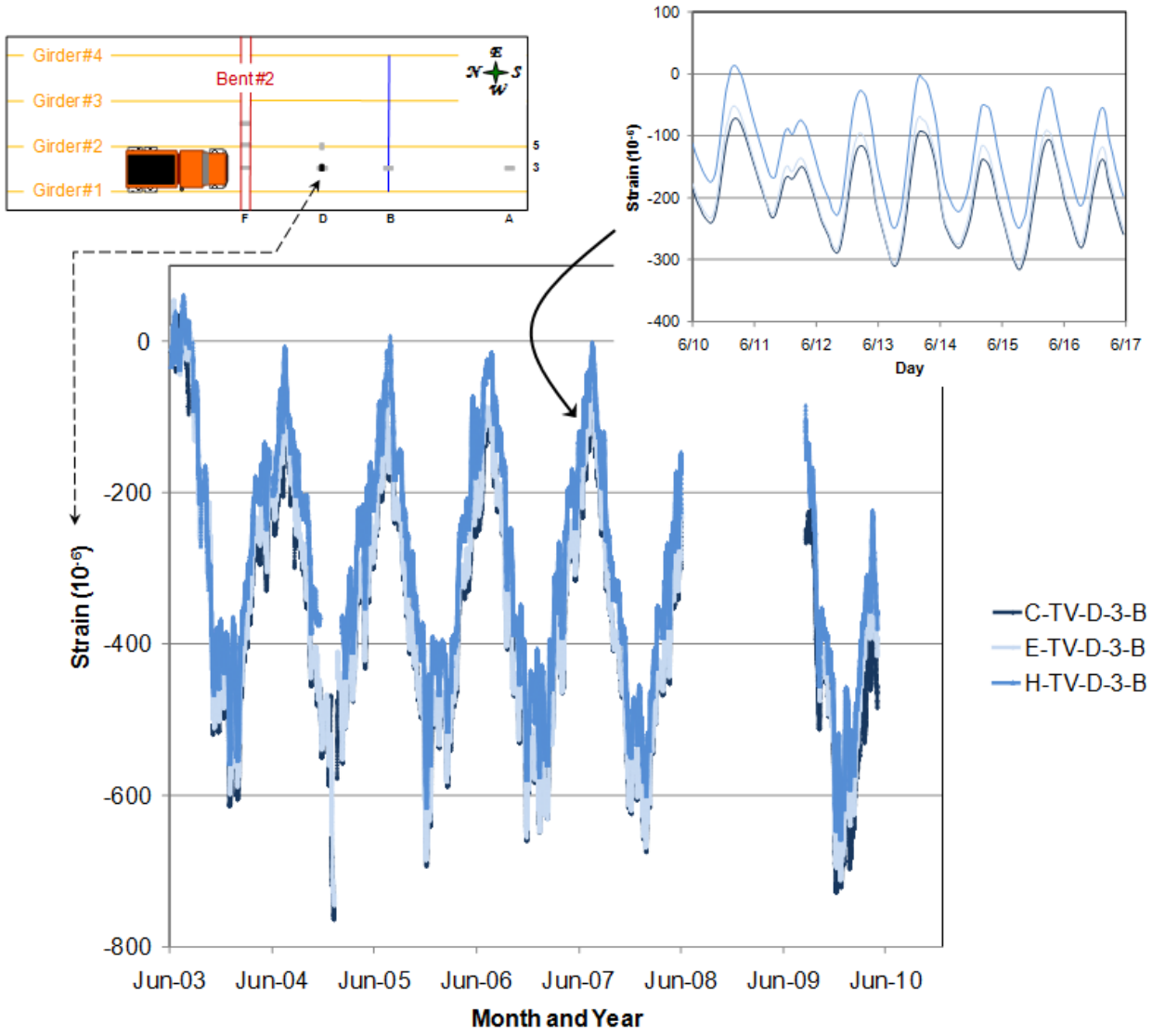

Figure 23: Strain history at all three bridge decks at gage location TV-D-3-B (smoothed).

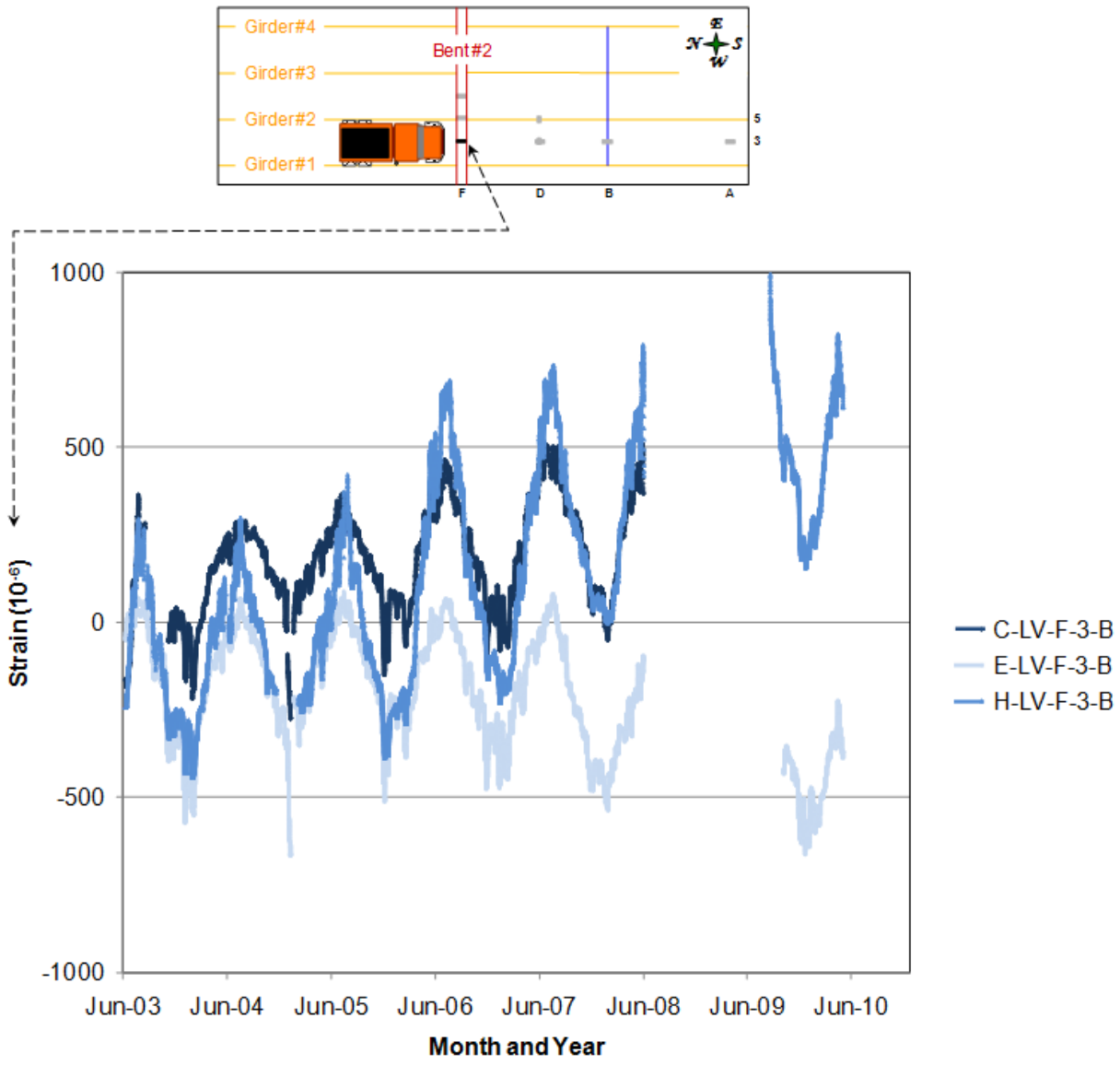

Figure 24: Strain history at all three bridge decks at gage location LV-F-3-B (smoothed).

Based on the general trends observed in the smoothed strain plots, the strain data was further analyzed by separating it into six time periods corresponding to their age. These time periods were used in comparative analyses to assess the changes within and between decks over time. The specific dates used for each time period for each deck are shown in Table 5. There are about 7,000 data points available for each time period for each bridge, although the exact number differs for each gage location. Data were available for the Conventional and HPC bridges for the Phase II study as early as August 28, 2009. However, data for the Empirical bridge deck were not available until October 15, 2009 due to technical difficulties with the data acquisition equipment. Data for the Conventional and HPC bridges were therefore truncated to match the Empirical bridge to allow for coincident comparisons to be made between the three structures.

Table 5: Time Periods Used for Comparative Analysis

Time Period	Age	CON	EMP	HPC
	Date Constructed	June 3, 2003	June 2, 2003	May 28, 2003
Year 1	28-days to 1 year	July 1, 2003 to June 3, 2004	June 30, 2003 to June 2, 2004	June 25, 2003 to May 28, 2004
Year 2*	1 to 2 years	June 3, 2004 to June 3, 2005	June 2, 2004 to June 2, 2005	May 28, 2004 to May 28, 2005
Year 3	2 to 3 years	June 3, 2005 to June 3, 2006	June 2, 2005 to June 2, 2006	May 28, 2005 to May 28, 2006
Year 4	3 to 4 years	June 3, 2006 to June 3, 2007	June 2, 2006 to June 2, 2007	May 28, 2006 to May 28, 2007
Year 5	4 to 5 years	June 3, 2007 to June 3, 2008	June 2, 2007 to June 2, 2008	May 28, 2007 to May 28, 2008
Year 7	6 to 7 years (7 month period)	October 15, 2009 to May 7, 2010	October 15, 2009 to May 7, 2010	October 15, 2009 to May 7, 2010

* The data acquisition system for the HPC deck experienced technical difficulties from November 16, 2004 to February 10, 2005. Thus data from the Conventional and Empirical decks were truncated to match the HPC decks.

To facilitate formulating quantitative comparisons of deck response, the overall response of the instrumented portions of the bridge decks was further characterized by averaging the responses from the vibrating wire strain gages across the various time intervals defined above, as well collectively across various orientations and locations within each deck (e.g., mean strain response of all transverse gages, all longitudinal gages, etc). The averaging process was expected to smooth out localized spatial and temporal variations in the collected data, and thus provide meaningful indicators of the broader long term response in a form conducive to conducting statistical characterization (and comparison) of this response. Variables that were investigated using this analysis included: deck type, time period, gage orientation, and gage line. The methodology and detailed results of these combinations of comparisons are described in more detail in Appendix C, and the significant findings are presented below.

In addition to mean strain response, the rate of change in the mean strain response over time was also of interest in studying the relative behavior of the decks. To determine this response parameter, the percent change between the strain response from a particular gage at two different time periods was computed (e.g., C-TV-A-3-B at a particular date and time in Year 1 compared to C-TV-A-3-B at that same date and time in Year 3). A single average value (and associated standard deviation) was then calculated from the thousands of values generated from these individual computations.

Box plots were produced from selected strain data to help identify locations where the bridge decks demonstrated noticeable differences in behavior. Box plots are a convenient way to view

large data sets, and more easily illustrate differences between data sets (here, the strain history for the three bridge decks) than other forms of statistical comparison. Box plots depict the lower quartile (25 percent of data are less than this value), median (half of data are greater than and half are less than this value), and upper quartile (75 percent of data are less than this value) in a box; lines above and below the box extend to the 90th and 10th percentile, respectively. A generic box plot labeled with the important features is presented in Figure 25. The mean (dashed line) is included to indicate its position in the data set relative to the median (solid line).

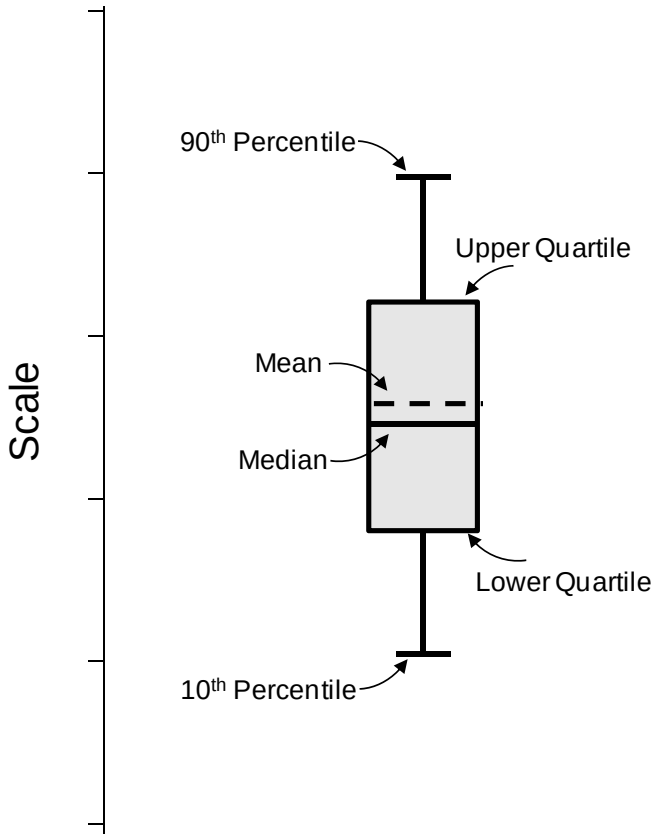

Figure 25: A generically labeled box plot.

While the box plots (and the graphs of the smoothed strain response) are useful in obtaining a general sense of possible differences between the response and condition of the three bridge decks, occasionally it was unclear whether any such observed differences were statistically significant or if more subtle differences, imperceptible using these visually based analysis techniques, were present. Thus, various quantitative statistical comparisons were made between the strain responses of the bridge decks using a two sample t-test. This test evaluates the statistical significance of the difference between the means of two sample populations (e.g., the difference in mean strain response observed in two bridges at gage line B in the longitudinal direction, or the difference in mean strain response for a single bridge observed during Year 3

and Year 7, etc.). The results of this test can be expressed in a variety of forms, and the decision was made to cite the p-value for each comparison. The p-value ranges between zero and one; values approaching zero indicate a greater likelihood that the sample means are different, while values approaching one indicate a greater likelihood that the means are the same. Another way to consider the p-value is by multiplying it by 100 to generate a percent. This percentage indicates the likelihood that the two means are equal when a random sample is chosen from each of the sample populations. For example, a p-value of 0.42 indicates that there is a 42 percent chance that the means are equal to one another.

5.2 Strain Response

There are fundamental differences in the expected structural behavior of a bridge deck in the transverse (perpendicular to the span) and longitudinal (parallel to the span) directions, as well as in the constraints offered in the two directions to shrinkage and temperature related deck movements. In the transverse direction, the decks are the primary structural element spanning between the girders, while in the longitudinal direction, the decks act in concert with the girders spanning between the abutments and bents. Restraint to in-plane shrinkage and temperature strains in the transverse direction is only nominally provided by the girders, while in the longitudinal direction the abutments and bents may offer considerable resistance to such strains. In light of these differences, the strain response was analyzed independently in the transverse and longitudinal directions. Further, this analysis focused on the deck responses along the A-, B- and D-lines. Data from the instrumentation along the F-line was generally neglected because the strain responses along this line near the south bent were known to be heavily influenced by local behaviors of the major transverse cracks that developed over the bents.

5.2.1 Transverse Strain Response

Transverse strains were available at positions D-5 and D-3 in each of the decks. In general, the strains at these two locations were similar to each other and similar between the three bridges, consisting of large seasonally related in-plane expansion and contraction of the decks (reaching -600 to -700 με in the winter, and returning to about 0 με in the summer) superimposed on a relatively constant shrinkage strain of approximately -350 με (negative signs indicate contraction). This strain is of the same order of magnitude as the shrinkage strain of -430 microstrain previously calculated for the decks using the AASHTO concrete shrinkage equation. Further, the magnitude of the seasonal strain cycles (600 to 700 microstrain) are generally consistent with the expected change in thermal strain calculated using the coefficient of thermal expansion of the deck concrete and the difference in temperature mid-summer to mid-winter temperatures. The distribution of strain through the depth of the deck at position D-3 was fairly uniform (indicating predominantly in-plane response), and showed the typical response to temperature and shrinkage described above (Figure 26).

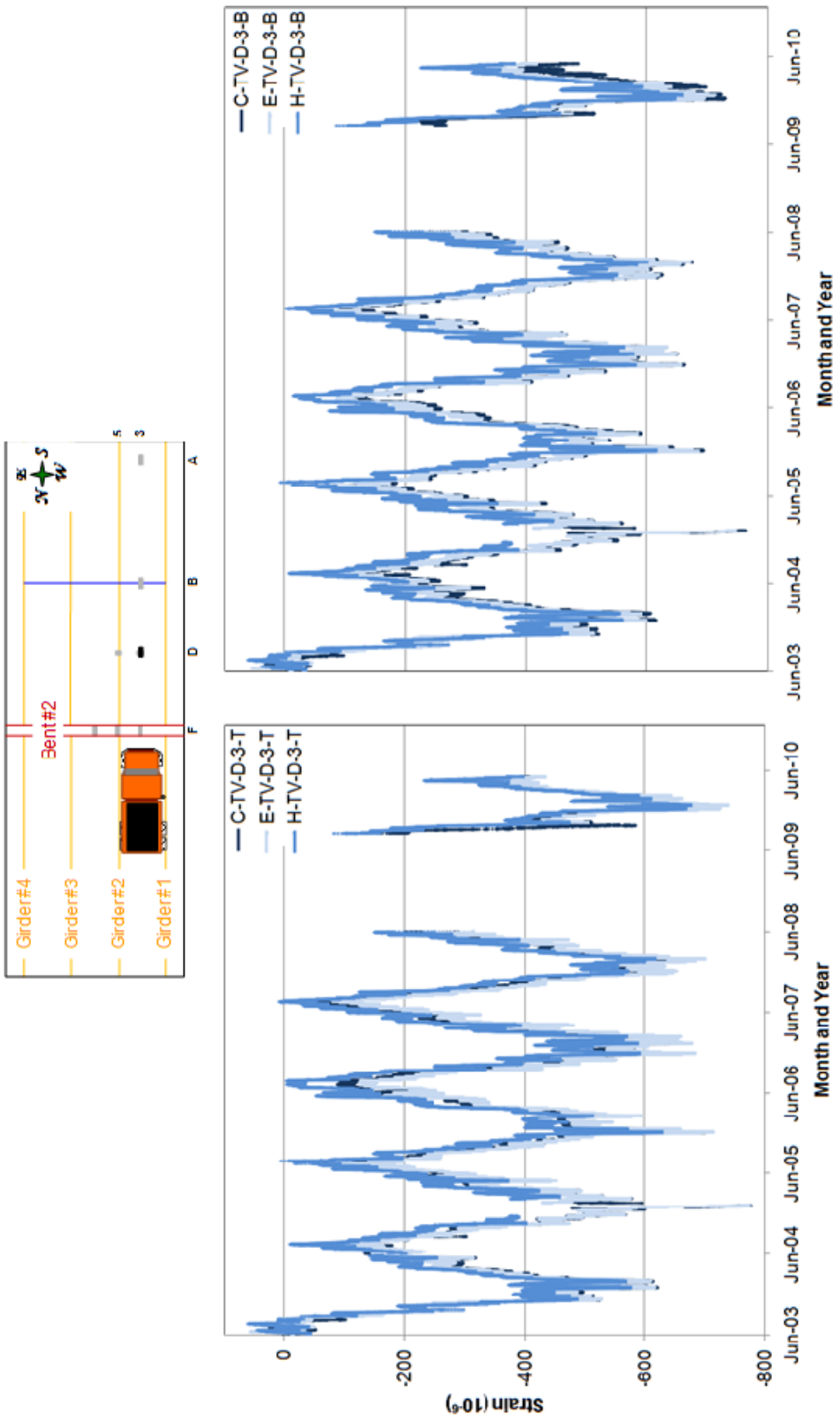

Figure 26: Strain in response at position D-3 near the top and bottom.

To represent the global behavior of the decks in the transverse direction, a single mean strain was calculated from all the data collected from the transverse gages (located at D-5 and D-3) throughout the monitoring period. The resulting mean transverse strain values were -370, -390, and -320 microstrain for the Conventional, Empirical, and HPC decks, respectively, as shown in the box plots in Figure 27. Statistical comparisons of these mean strains showed that the HPC deck was dissimilar to the other decks (p-values of 0.31 and 0.11 when compared to the Conventional and Empirical decks, respectively, as presented in Table 6). In other words, the p-values indicate in this case that the mean strain response in the HPC and Conventional decks have a 31 percent chance of being the same (p = 0.31), and the mean responses of the HPC and Empirical decks only have an 11 percent probability of being the same (p = 0.11). A further statistical analysis of the mean transverse strain by individual years (Table 7) showed the mean strains were most similar during Year 1, and that the Empirical and HPC decks are the least similar to one another from Year 2 through Year 7. Overall, this analysis showed that the magnitude of the mean strain in the transverse direction is lowest in the HPC deck, which corresponds to shrinkage measurements made on collected concrete samples, and the mean strain in the transverse direction is similar in the Empirical and Conventional decks, which are both higher than in the HPC deck.

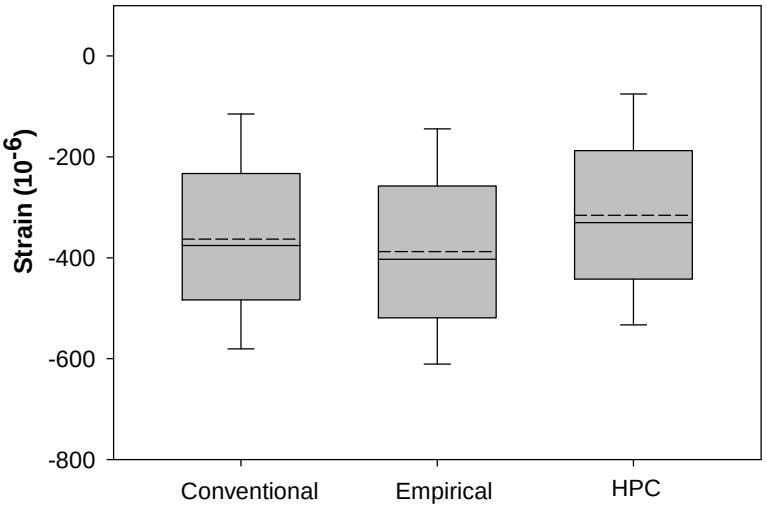

Figure 27: Box plots for each deck based on strain from all transverse gages.

Table 6: P-values for all Transverse Strain Gages

Orientation	Comparison	P-value
Transverse	CON-EMP	0.65
	CON-HPC	0.31
	EMP-HPC	0.11

Table 7. P-values for Time-Separated Transverse Strains

Orientation	Year	Comparison	P-value
Transverse	1	CON-EMP	0.81
		CON-HPC	0.65
		EMP-HPC	0.81
	2	CON-EMP	0.93
		CON-HPC	0.43
		EMP-HPC	0.34
	3	CON-EMP	0.81
		CON-HPC	0.68
		EMP-HPC	0.46
	4	CON-EMP	0.78
		CON-HPC	0.64
		EMP-HPC	0.40
	5	CON-EMP	0.79
		CON-HPC	0.69
		EMP-HPC	0.47
	7	CON-EMP	0.71
		CON-HPC	0.85
		EMP-HPC	0.47

The transverse strains were also analyzed to assess the rate of change in the mean response from Year 1 to Year 3 to Year 7, as described above. If a particular deck exhibited a reduction in the rate of change of strain relative to the other decks, this would indicate a relative stabilization in its behavior, which in turn could be related to an extension in its service life with respect to the other decks. Referring to the box plot in Figure 28, the average percent change in strain from Year 1 to Year 3 was slightly higher than from Year 3 to Year 7 in the Conventional and Empirical decks, and similar in both time periods for the HPC deck, but the data "boxes" in all cases overlap significantly. Even at seven years of age, the bridge decks are still relatively young, and it is more logical to assess the rate of change in the strains over the entire 7 year period rather than the shorter periods. As such, the average percent change from Year 1 to Year 7 was around 30 percent (Table 8). The p-values associated with the comparisons of these mean rates of change are all above 0.9, indicating that they were all very similar to one another.

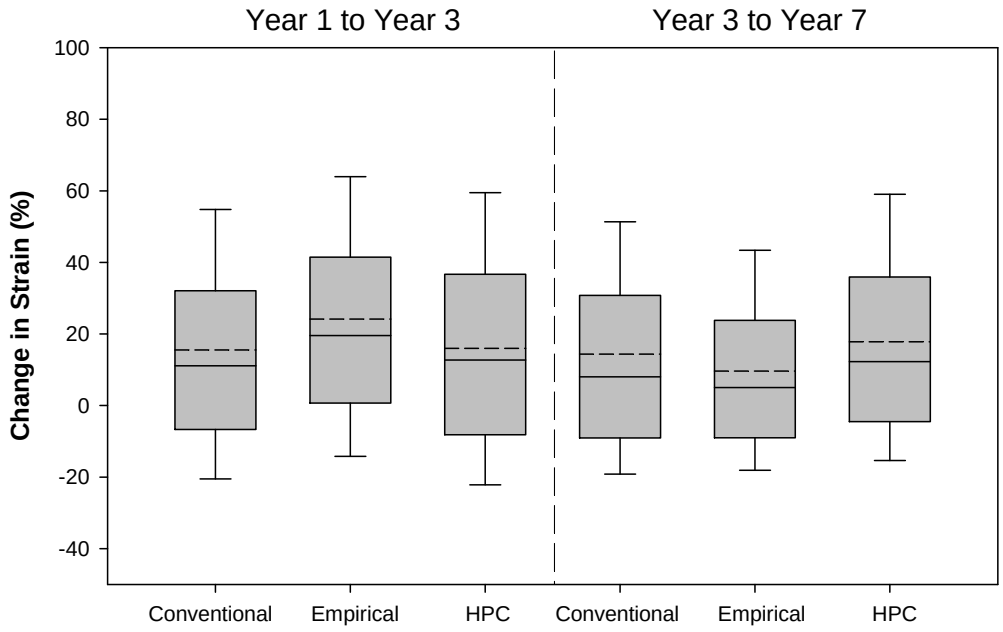

Figure 28: Box plot of the percent change over time between the transverse gages.

Table 8: Mean Percent Change in Strain for Transverse Gages

Orientation	Year	Bridge	Mean
Transverse	1 to 7	CON	28
		EMP	32
		HPC	30

5.2.2 Longitudinal Strain Response

Longitudinal strains in the bridge deck were measured at transverse gage lines A, B and D along longitudinal gage line 3 between the girders (i.e., A-3, B-3 and D-3). The general longitudinal strain response has the same prominent features as in the transverse direction, with large seasonally related expansion and contraction (reaching -600 to -700 με in the winter and returning to about -100 με in the summer) superimposed on a shrinkage strain of approximately -400 με (Figure 29).

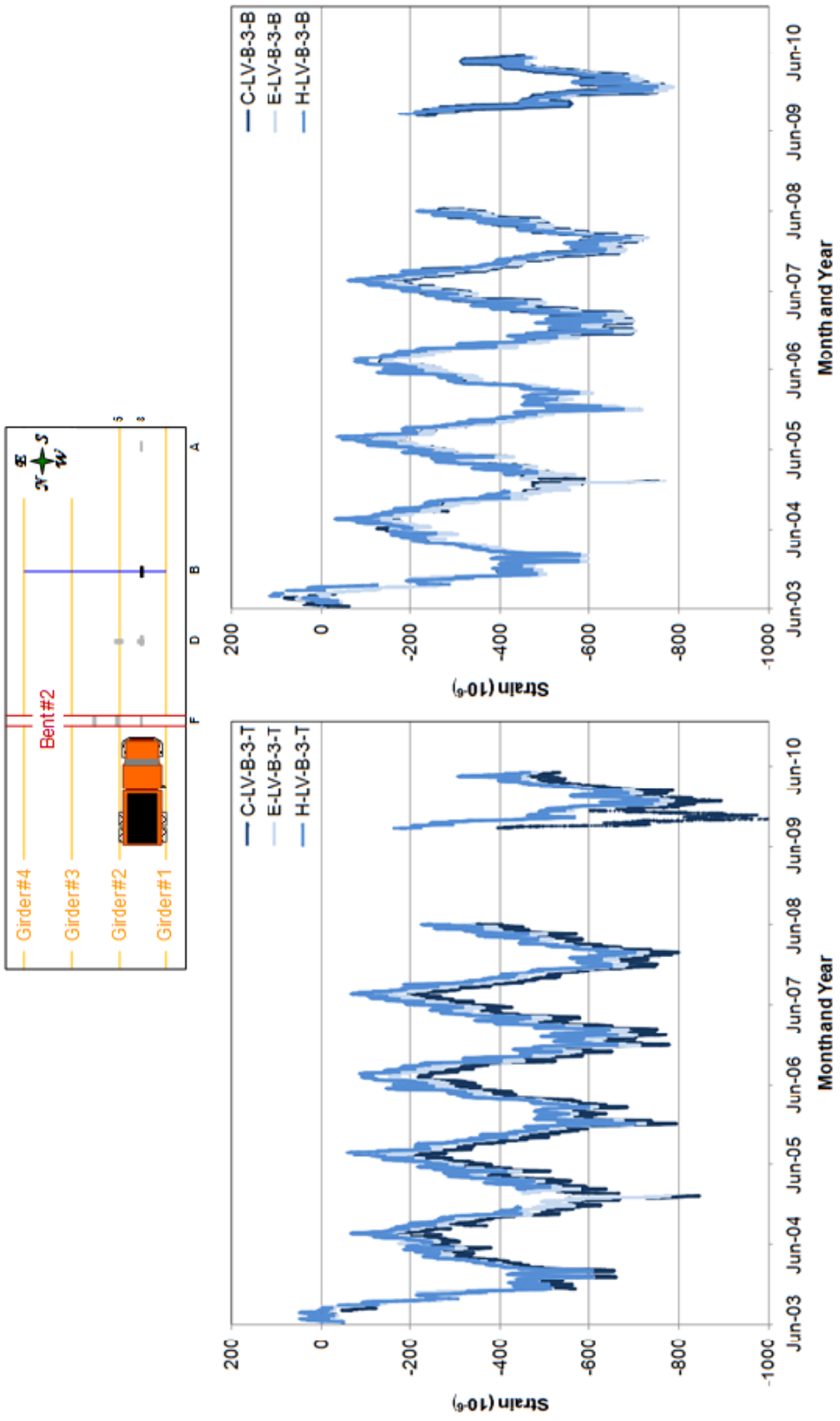

Figure 29: Strain response at position B-3 near the top and bottom of the deck oriented longitudinally.

In the longitudinal direction a mean strain analysis was also conducted to investigate possible subtle differences in behavior between the bridge decks not apparent in the qualitative visual comparison provided in Figure 29. The mean strain responses calculated from all the longitudinal gages (from the A-, B- and D-lines, and not the F-line) in each deck for the entire data monitoring period were about -310 to -390 με in magnitude and ranged from about -160 to -510 με, as shown in Figure 30. A statistical analysis of these means, however, found that the p-values associated with these comparisons are all lower than 0.5, as shown in Table 9. When a more specific analysis was done with respect to gage line, the differences in the mean values were found to be most clearly evident in the A-line (Table 10), where it was seen that the Empirical deck was clearly different than the Conventional and HPC decks (p-values = 0.01 and 0.03, respectively). As previously described, values along the F-line were not included in the global analysis because the behaviors in this area were known to be heavily influenced by transverse cracking in the decks coincident with the intermediate support and, therefore, may not be representative of global deck behaviors. The p-values associated with the strain measurements taken along the F-line are shown in Table 10.

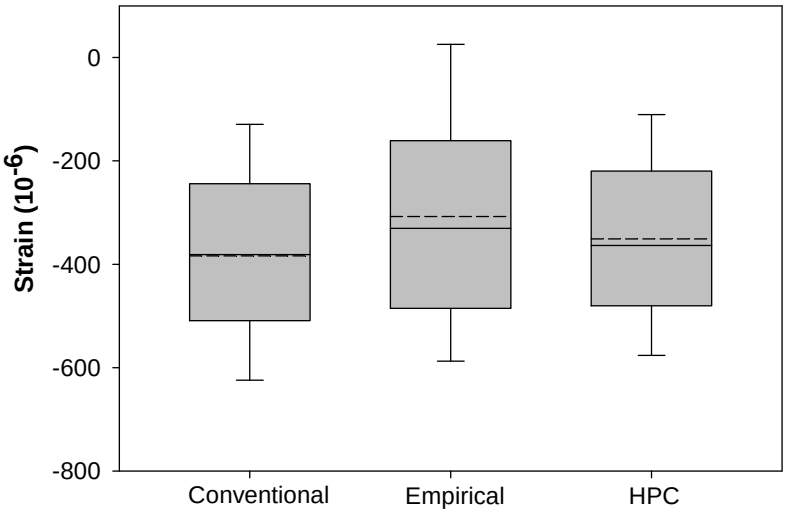

Figure 30: Box plots for each deck based on strain from all longitudinal gages.

Table 9: P-values for Longitudinal Strain Gages

Orientation	Comparison	P-value
Longitudinal	CON-EMP	0.16
	CON-HPC	0.49
	EMP-HPC	0.39

Table 10: P-values for Gage-Line Separated Longitudinal Strains

Line	Comparison	P-value
A	CON-EMP	0.01
	CON-HPC	0.69
	EMP-HPC	0.03
B	CON-EMP	0.58
	CON-HPC	0.34
	EMP-HPC	0.67
D	CON-EMP	0.61
	CON-HPC	0.89
	EMP-HPC	0.65
F	CON-EMP	0.00
	CON-HPC	0.00
	EMP-HPC	0.68

The comparison of the typical responses in the transverse and longitudinal directions revealed a noticeable and continuous decrease in the magnitude of the mean longitudinal strains over time (compare Figure 26 to Figure 29). The cause for this gradual and continuing increase in deck contraction in the longitudinal direction over time is uncertain, although deck shrinkage in the longitudinal direction will be affected by the girders, which may be shrinking more slowly than the deck above primarily due to their sheltered position under the deck. The rate of change in the mean strains was evaluated to determine the significance of this difference. This analysis revealed that the rate of change in the mean strains in the longitudinal direction appeared to be greater between Year 1 and Year 3 than between Year 3 and Year 7, as illustrated in Figure 31. The mean percent changes over the entire evaluation period (Year 1 to Year 7) were relatively similar between decks—55 percent for the Conventional and HPC decks and 49 percent for the Empirical deck (Table 11). The p-values associated with the comparison of these mean rates of change are greater than 0.9 indicating that the rates of change within the decks were similar. Overall, greater changes occurred in the longitudinal relative to the transverse strains (approximately 50 percent compared to 30 percent, respectively).

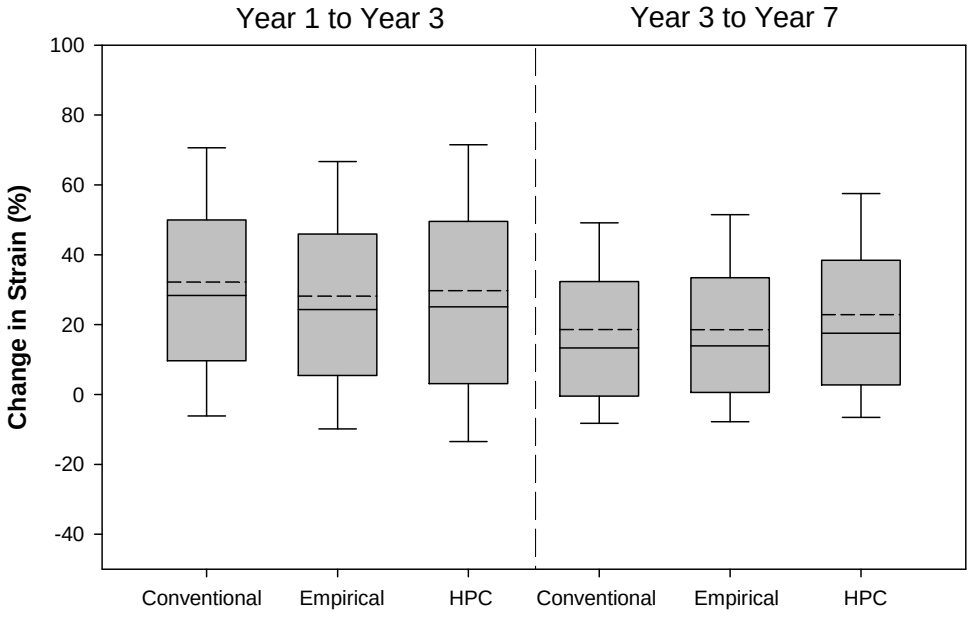

Figure 31: Box plot of the percent change over time between the longitudinal gages.

Table 11: Mean Percent Change in Strain for Longitudinal Gages

Orientation	Year	Bridge	Mean
Longitudinal	1 to 7	CON	55
		EMP	49
		HPC	55

The A-line was instrumented with two longitudinal gages: one near the top of the deck and one near the bottom. While the strain responses at LV-A-3-T were similar between the three decks, the strain response for the bottom gage (LV-A-3-B) was different in the Empirical deck, as illustrated in Figure 32 and Figure 33. The p-values all increase to values greater than 0.5 (Table 12) when the strains associated with gage A-3-B are removed from the analysis. The strains in the Empirical deck are routinely expansive at LV-A-3-B in the summer, with peaks above 300 με. In addition, the visual distress survey revealed a hairline crack on the underside of the Empirical deck in the vicinity of A-3-B, which may have developed due to these tensile strains. Differences at this location within the Empirical deck may be due to the behavior of the integral abutment in this region.

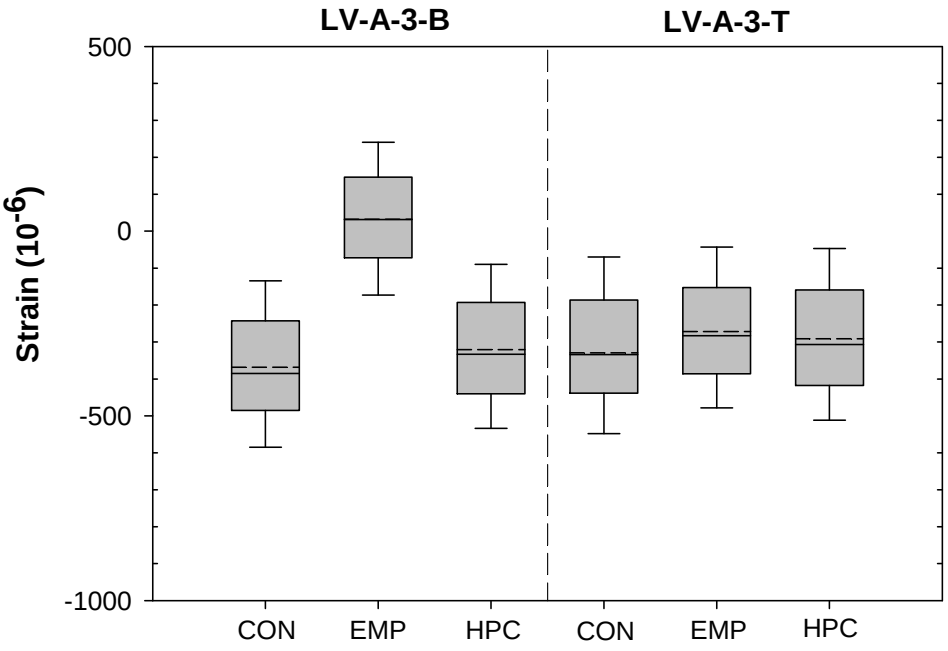

Figure 32: Box plots for longitudinal gages at the A-line.

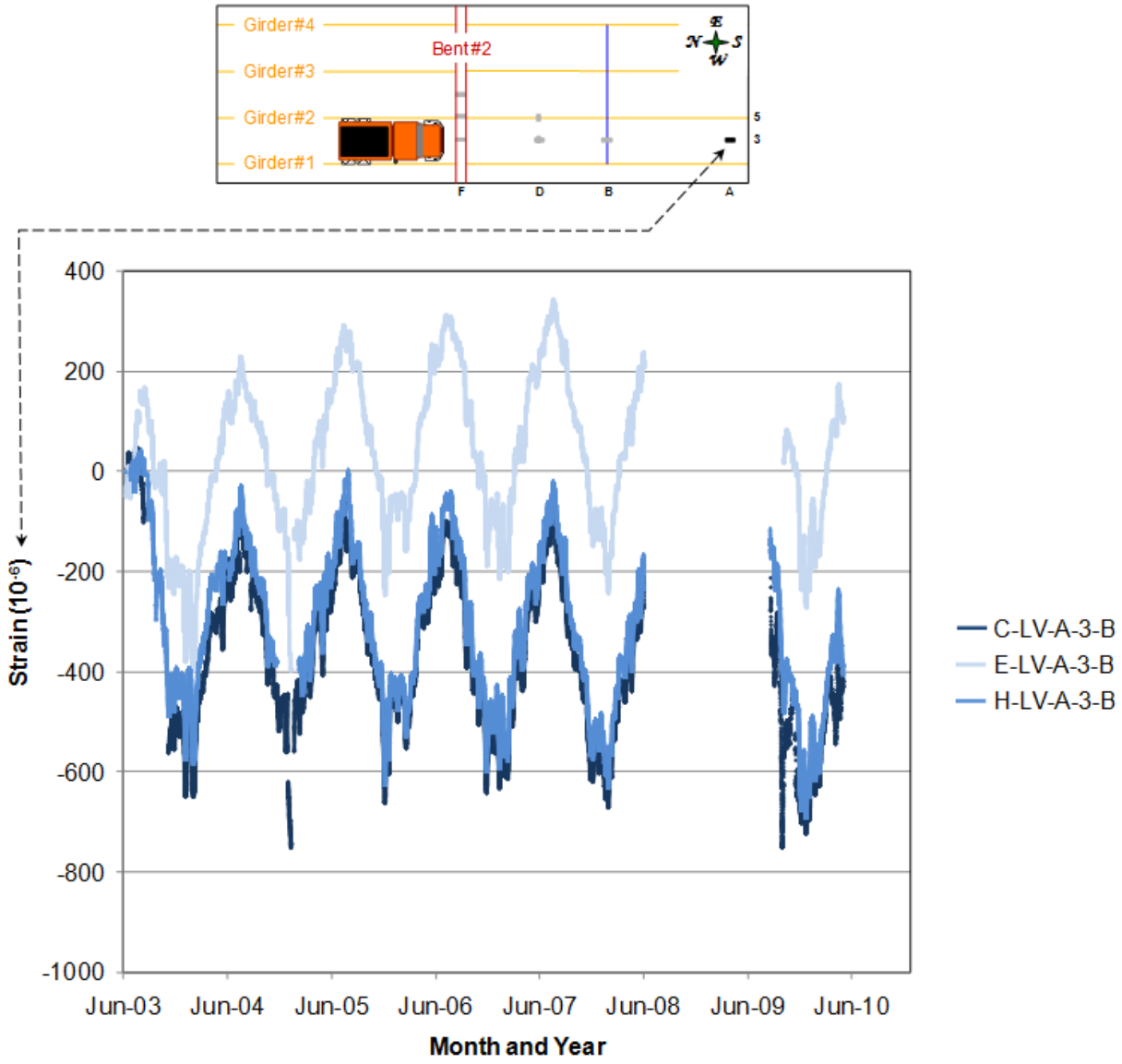

Figure 33. Strain history at all three bridge decks for longitudinal gage located at A-3-B (smoothed).

Table 12: P-Values for Longitudinal Strain Gages without A-3-B

Orientation	Comparison	P-value
Longitudinal	CON-EMP	0.88
	CON-HPC	0.58
	EMP-HPC	0.66

5.3 Summary

Strain gages installed in the bridge decks during construction were monitored from summer 2003 to summer 2008 and from fall 2009 to spring 2010. The focus of this study was on the long-term

response in the bridge decks to environmental conditions—primarily temperature and shrinkage. In general, the decks are all responding similarly, where this response consists of temperature related diurnal strain cycles superimposed on temperature related seasonal strain cycles, all of which are superimposed on long term shrinkage strains. The mean strain response was characterized for both the transverse and longitudinal directions. In the transverse direction, the mean strain in the HPC deck was less than the mean strains in the Conventional and Empirical decks. This is not surprising as the shrinkage strains measured in concrete samples collected during deck construction revealed lower shrinkage strains in the HPC deck concrete. The rate of change of the mean transverse strains in all three decks are slowing slightly over time and are similar in magnitude, indicating that the behavior of no one deck is stabilizing more rapidly than the other decks. In the longitudinal direction, the mean strains in the decks were least similar to each other near the abutment and over the bent. Away from these features, the responses were generally similar. The differences between the bridges observed near the abutment are heavily influenced by the local behaviors associated, perhaps, with the behavior of the integral abutment, as determined by the strain response in the Empirical deck at location A-3-B and evidenced by the transverse crack on the bottom surface near that strain measurement location.

6 COST ANALYSIS

To conduct a meaningful life-cycle cost analysis of the decks, construction, maintenance, repair and rehabilitation cost data are necessary. This information is matched against the level of service they offer and their useful life in completing the life-cycle cost analysis. Construction costs for the Saco bridge decks were well documented in the initial study at $57,672 for the Conventional and HPC decks, and $52,172 for the Empirical deck. No significant additional maintenance activities have been conducted since completion of the bridges. Relative to their present serviceability and expected life, only small differences have been observed in the condition of the decks since being placed into service, and these differences are insufficient to confidently predict any attendant differences in their expected service lives. Even though the HPC deck appears to be nominally performing better than the other two decks at this time, it still is difficult to determine what if any enduring long term benefit may be realized with this deck, and whether the quantitative magnitude of this benefit will be commensurate with its increased initial cost. Thus, future monitoring of the bridge decks, as well as costs and timing associated with maintenance, repair and rehabilitation are needed to determine the cost-benefit ratio for each bridge deck design type.

7 CONCLUSIONS AND RECOMMENDATIONS

The baseline analysis conducted during the first phase of this project established the baseline condition of the three bridge decks prior to extensive demands from traffic and the environment. Data obtained from continued long-term monitoring has furthered the body of evidence from which to make judgments about which deck design offers superior performance. The primary conclusion from the analysis of the long-term data collected during the past seven years is that the three bridge decks are still performing well and relatively similarly to one another. Nevertheless, based on all of the information obtained to date, the HPC deck seems to be performing slightly better than the other two decks. This conclusion is based on 1) less severity and lower quantity of deck cracking, and 2) lower long-term strain magnitudes due to less shrinkage of the deck concrete. The greatest changes occurred in the Conventional deck during the past five years—its performance now corresponding more closely to the Empirical deck. Other minor differences are apparent from the analysis conducted as part of this research. These differences were noted with respect to the visual distress surveys, corrosion testing, shrinkage measurements, and long-term strain analysis. Specific observations from each of these assessments are listed below.

- Half cell testing indicated very little potential for corrosion of the deck reinforcement, nor did it reveal any differences between the decks.
- Other than some longitudinal tilting of the structures, differential movement of the decks was relatively small (on the order of 1 to 5 mm across the length of the deck), based on the topographic surveys.
- A comparison between the three decks generally indicated that cracking near the abutments and over the bents was most pronounced in the Conventional and Empirical decks, and that these distresses were very similar in these two decks.
- From the visual distress data collected thus far, it appears that the HPC deck is performing somewhat better than the other two decks.
- The HPC and Conventional decks had a greater number of hairline cracks on the underside of the deck when compared to the Empirical deck.
- Measurements of HPC deck concrete samples indicated shrinkage of this concrete was less than the conventional concrete, which was used in both the Conventional and Empirical decks.
- The magnitudes of the mean strain in the transverse direction (based on gage locations D-3 and D-5) indicate that the decks have contracted, which corresponds to shrinkage measurements made on collected concrete samples. The mean strains in the transverse direction are similar to one another in the Empirical and Conventional decks, and are slightly greater than the mean strains in the HPC deck.

- The rate of change in average strain in the transverse and longitudinal directions over time was similar in the three decks. The magnitudes of the mean strain in the longitudinal direction (based on gage locations A-3, B-3 and D-3) also indicate the deck has contracted, corresponding to shrinkage in the deck concrete similar in magnitude to the mean strain levels in the transverse direction.
- Statistically significant differences were found in the mean strain in the longitudinal direction between the bridges, although these differences were primarily caused by greater strains in the Empirical deck at gage position A-3-B near the abutment.

7.1 Recommendations

The extensive monitoring programs carried out on the Saco bridges during the initial study and this seven-year review have expanded the knowledge of the behavior of the three types of bridge decks over time. The question of which of the three bridge deck designs may offer the best life cycle performance, however, remains unresolved; the three bridges are relatively young, and any significant behavioral and performance differences between the decks have not yet manifested themselves. Thus, as was concluded following the first project, it is recommended that monitoring of the structures be continued. The overall objective of this continued monitoring is to document and understand if and when significant differences in deck behavior occur, at which time a more definitive assessment of cost benefit by deck type can be completed. Four main activities are recommended to further study these structures: long-term monitoring, live load testing, finite element analysis, and laboratory exploration. Each of these efforts is developed in greater detail below.

7.1.1 Long Term Monitoring

Long term monitoring is crucial to understand and quantify potential differences in the behavior of these three structures over time. Much more can be learned in the future by capitalizing on the instrumentation infrastructure and analytical methodologies already established. The analysis performed for this project utilized data collected since the bridges were constructed (2003 to present), and included considerable data collected when there was no active project to support this activity. This added data allowed a more complete analysis to be conducted in this project of the deck responses over time. Therefore, it is recommended that the vibrating wire strain gages continue to be monitored over time. This could be efficiently accomplished by simplifying the datalogger wiring and programming to monitor only the vibrating wire strain gages and companion temperatures. The vibrating wire gages continue to work well and data could continue to be collected and stored with little effort and cost. Data from the sensors can be analyzed in a similar manner as described in this report at a later date (for example, when the bridges are 10 to 15 years old).

The material testing, topographic surveys, and visual distress surveys also provided critical information about the relative performance of the bridge decks. As such, the following items should continue to be monitored on a periodic basis (say, biennially):

- visual distresses, to document the formation of cracks, delaminations, and settlement of the bridge approaches;
- corrosion tests, to detect possible deterioration of the reinforcement and concrete;
- deck elevations, to monitor global movements of the structures, and
- maintenance costs, to evaluate the cost effectiveness of each deck type.

7.1.2 Live Load Tests

Live load tests are also vital to evaluate the performance and behavior of the decks under vehicle loading with the ultimate goal of quantifying crack potential, and comparing performance and/or condition based on potential damage indicators such as deck stiffness and validity of superposition. It is recommended that live load tests be conducted in the future when the decks reach a certain age (perhaps 10 to 15 years old) or when there are significant changes in the deterioration or strain levels within the decks based on long term monitoring. By continuing to collect this information over time, even subtle changes in condition will be captured and documented. Furthermore, this data will help determine the cause of more significant distresses, if and when they occur. The electrical resistance strain gages attached to the reinforcement and embedded in concrete were used in the live load tests conducted during the initial study. These gages have mostly reached their life expectancy, but live load testing is possible using the vibrating wire sensors by step-wise moving a loaded vehicle across the bridge and taking static strain measurements at each vehicle position, rather than using dynamic moving loads (as was done in the first phase of this study). Alternatively, recent advances in data acquisition equipment currently being developed may allow dynamic responses to be obtained from vibrating wire strain gages.

7.1.3 Finite Element Modeling

This project has documented the behavior of the three decks over the past seven years. There are still many unknowns regarding the behavior of certain components of these bridges (e.g., the concentration of cracking near the integral abutments). Finite element analysis can help study particular behaviors and/or measured responses thought to affect the overall performance of each bridge deck type.

7.1.4 Laboratory Study

During the course of the initial research project, several laboratory studies were conducted to evaluate certain aspects of material and deck performance in a controlled environment. In one laboratory study, a scale model of a transverse section of the bridge deck was built and instrumented with the same sensors as were used in the three bridges in Saco. This model was then subjected to static loads while each of the sensors was monitored. In addition, it was stored outside to experience daily and seasonal temperature cycles—similar to the Saco bridges. Further testing of this beam would help understand transverse behaviors of the bridge decks in Saco, sensor drift, and the effects of temperature on sensor function. A new climate controlled

laboratory at Montana State University (Subzero Science and Engineering Research Laboratory) will also allow this type of physical model to be tested at a variety of environments and temperatures.

8 REFERENCES

AASHTO (2000) LRFD Bridge Design Specifications, 2nd ed., American Association of State Highway and Transportation Officials, Washington, D.C.

ACI (2008) Report 209R2-08 Guide for Modeling and Calculating Shrinkage and Creep of Hardened Concrete, Reported by ACI Committee 209, Farmington Hills, MI.

Cuelho, E.V., J. Stephens, P. Smolenski, and J. Johnson (2006) Evaluating Concrete Bridge Deck Performance. Montana Department of Transportation, Final Report No. FHWA/MT-06-006/8156-002.

Johnson, J. (2005) "Concrete Bridge Deck Behavior Under Thermal Loads," Thesis submitted to Montana State University for the fulfillment of a Master's degree in Civil Engineering, Bozeman, MT.

Russell, H.G., R.A. Miller, H.C. Ozyildirim, and M.K. Tadros (2006) Compilation and Evaluation of results from High-Performance Concrete Bridge Projects. Federal Highway Administration, Final Report No. FHWA-HRT-05-057.

Zia, P., A. Shuaib, and M. Leming (1997) High-Performance Concretes: A State-of-Art Report (1989-1994). Federal Highway Administration, Report No. FHWA-RD-97-030.

Appendix A:
List of Failed Gages

Legend:

As of May 2004
As of July 2005
As of October 2009

Conventional Deck		
Resistance	Embedded	Vibrating
C-LR-B-5-T	C-LE-F-5-M	C-TV-D-5-M
C-LR-F-3-T	C-LE-F-5-T	C-LV-F-5-M
C-LR-F-5-T	C-LE-F-7-M	C-LV-F-5-T
C-LR-G-5-T	C-LE-F-7-T	C-LV-F-3-B
C-LR-B-3-B	C-TE-D-2-T	C-LV-F-3-M
C-LR-B-1-T	C-TE-D-5-T	C-LV-F-3-T
C-LR-D-3-T		C-LV-D-3-B
C-LR-B-3-T		C-LV-D-3-T
C-TR-D-1-B		C-TV-D-5-B
C-TR-D-5-T		C-LV-A-3-T
C-TR-D-1-T		
C-TR-D-4-T		
C-LR-D-5-T		
C-TR-D-6-T		
C-TR-E-5-T		
C-LR-F-7-T		
C-LR-F-1-B		
C-LR-A-3-T		
C-TR-B-2-T		
C-LR-C-3-T		
C-TR-D-2-T		
C-TR-E-5-B		
C-LR-F-7-B		
C-LR-F-3-B		
C-LR-F-1-T		

Empirical Deck		
Resistance	Embedded	Vibrating
E-LR-F-1-B	E-LE-F-5-M	E-LV-F-5-B
E-TR-D-1-T	E-LE-F-5-T	E-LV-F-5-T
E-LR-F-3-T	E-LE-F-7-T	E-LV-F-7-B
E-LR-C-3-T	E-LE-F-7-M	
E-TR-D-6-T		
E-LR-B-5-T		
E-LR-D-3-T		
E-LR-B-3-T		
E-TR-D-5-B		
E-TR-D-6-B		
E-LR-B-1-T		
E-LR-B-3-B		
E-LR-A-3-T		
E-LR-F-7-T		
E-LR-G-5-T		
E-LR-F-7-B		
E-LR-F-3-B		
E-TR-E-5-T		
E-TR-D-5-T		
E-TR-D-2-T		

HPC Deck		
Resistance	Embedded	Vibrating
H-LR-F-7-T	H-LE-F-5-T	
H-LR-B-3-T	H-LE-F-7-M	
H-LR-F-5-T	H-LE-F-5-B	
H-TR-D-5-B	H-LE-F-7-T	
H-LR-A-3-T	H-LE-F-5-M	
H-LR-B-1-T	H-TE-D-5-T	
H-LR-B-5-T	H-TE-D-2-T	
H-TR-B-2-T		
H-TR-B-2-B		
H-LR-B-3-B		
H-LR-C-3-T		
H-TR-D-5-T		
H-TR-D-2-T		
H-TR-D-6-T		
H-TR-D-1-B		
H-LR-D-3-B		
H-TR-D-4-T		
H-TR-D-1-T		
H-LR-D-5-T		
H-TR-D-6-B		
H-TR-E-5-T		
H-TR-E-2-T		
H-LR-F-3-T		
H-LR-G-5-T		
H-LR-D-3-T		
H-TR-E-5-B		
H-LR-F-1-B		
H-LR-F-7-B		
H-LR-F-3-B		

Appendix B:
Smoothed Strain Response Plots

LIST OF FIGURES

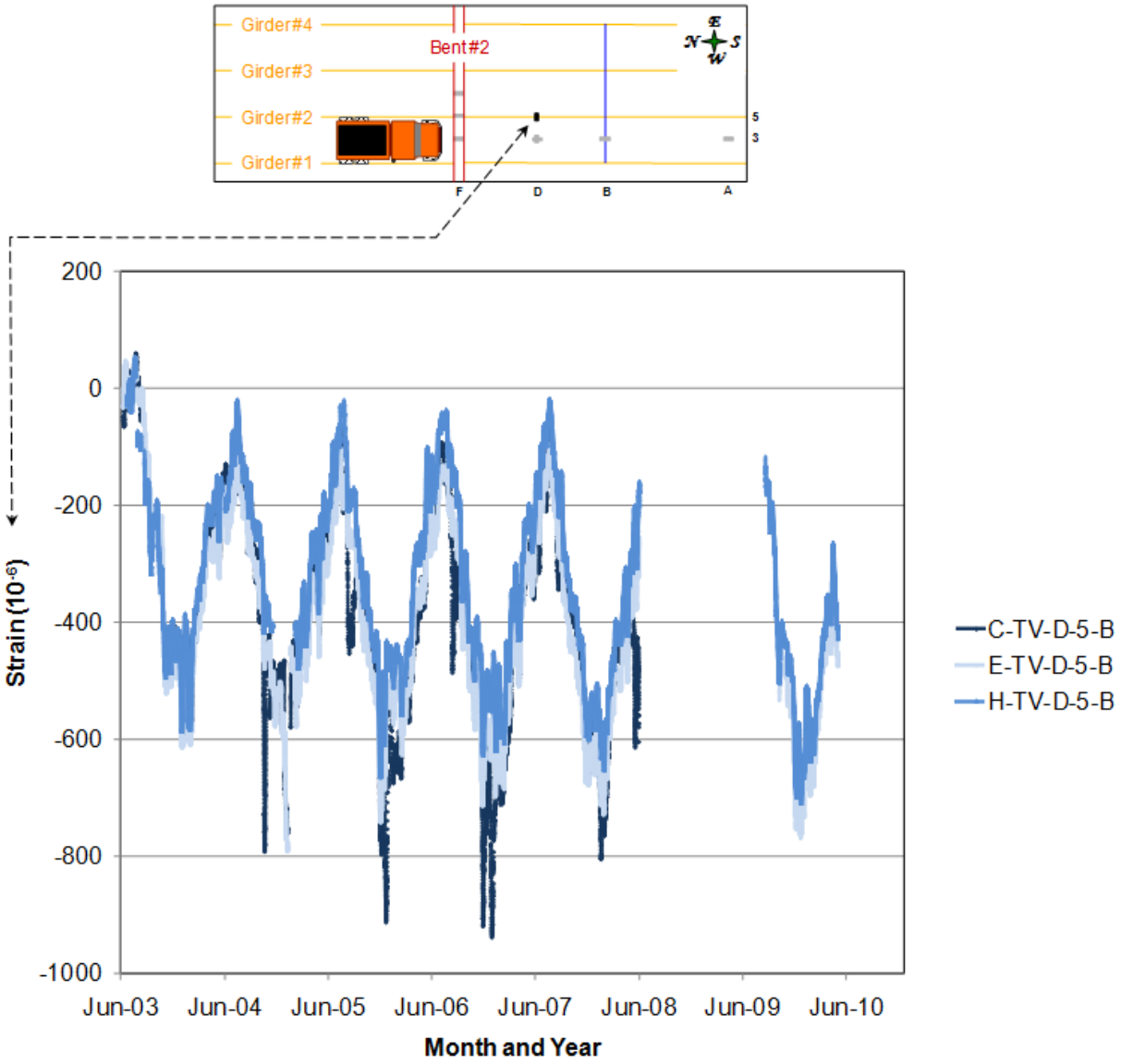

Figure B-1: Smoothed, transverse strain history at gage location D-5-B.

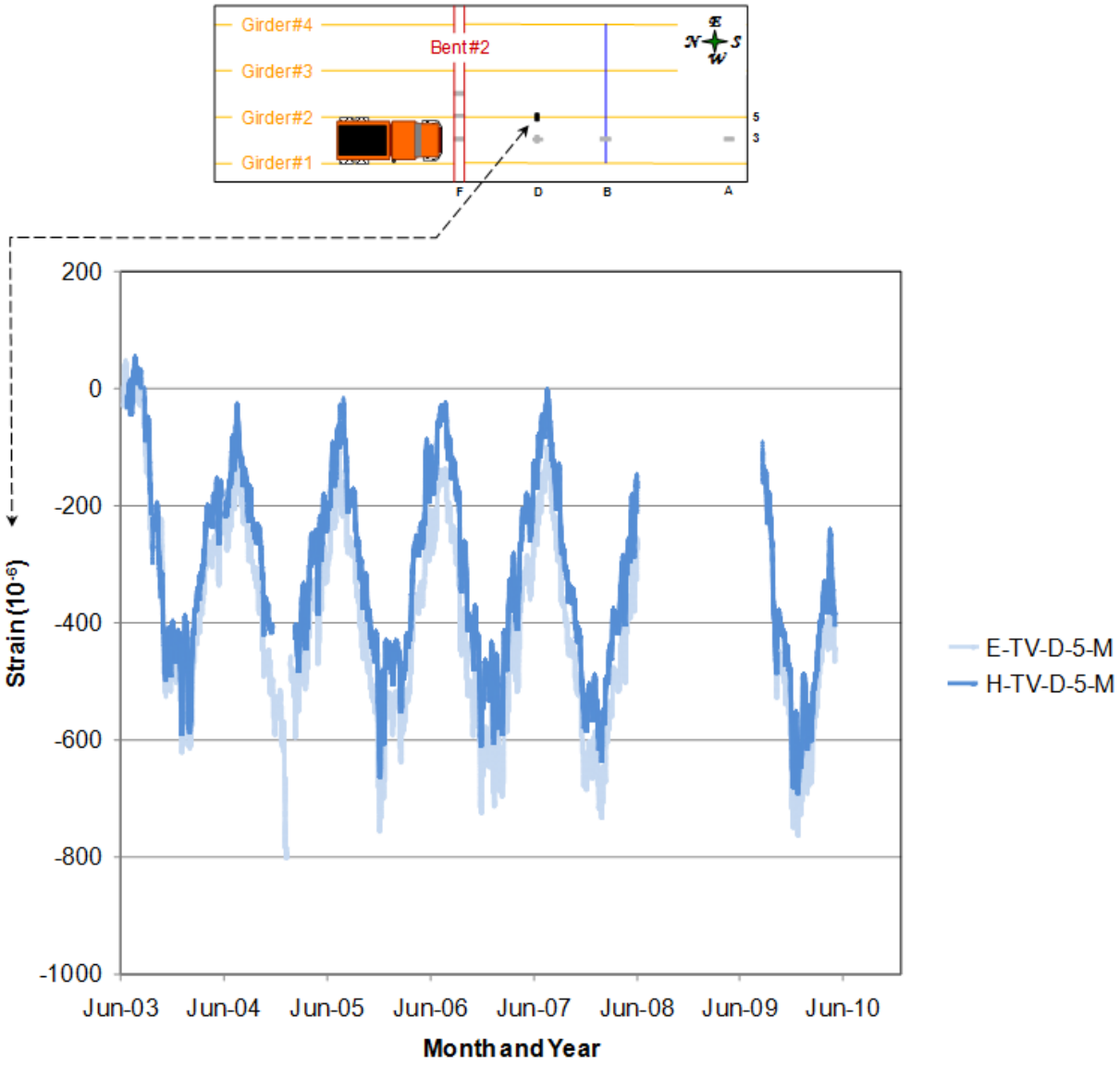

Figure B-2: Smoothed, transverse strain history at gage location D-5-M.

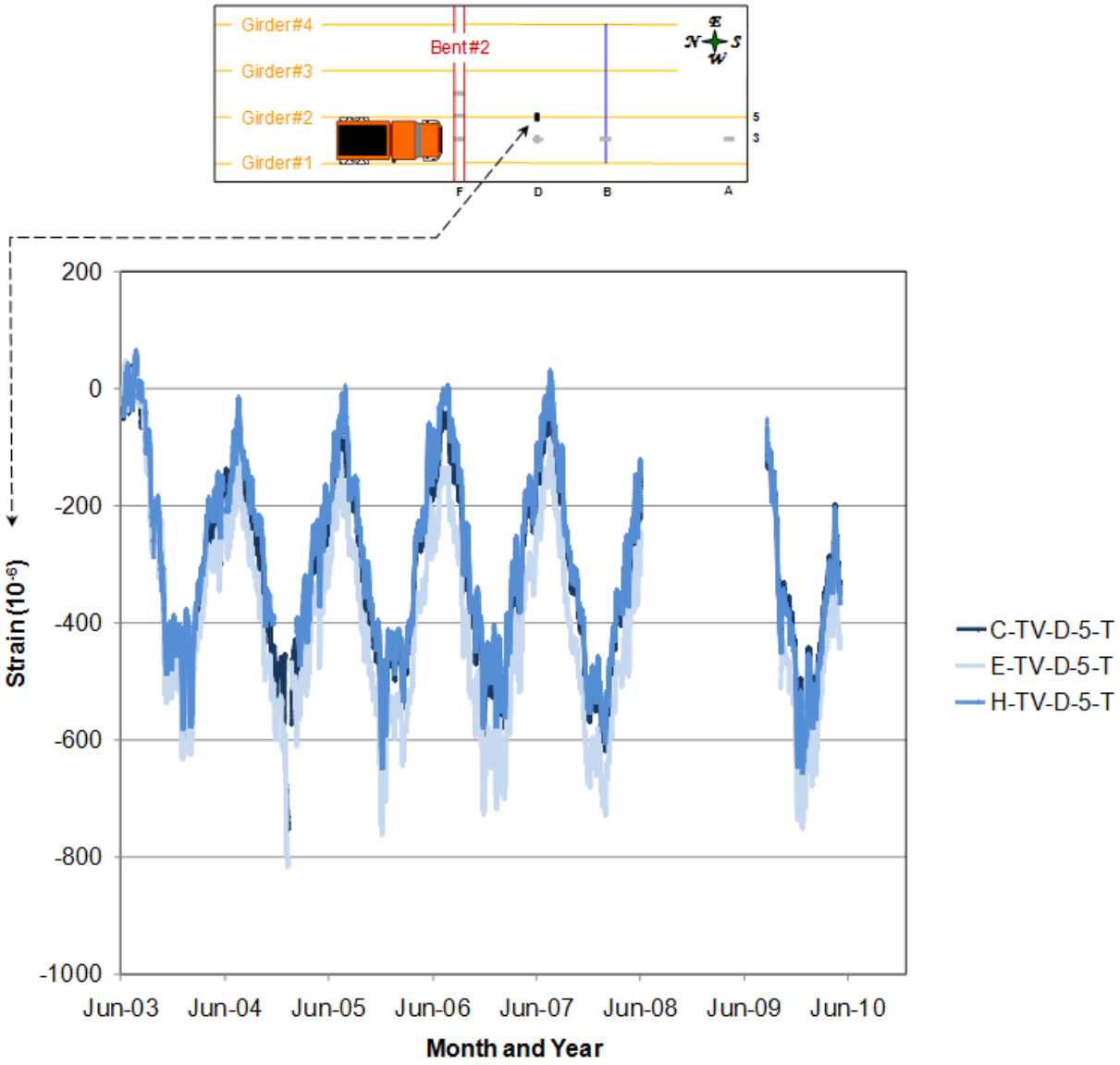

Figure B-3: Smoothed, transverse strain history at gage location D-5-T.

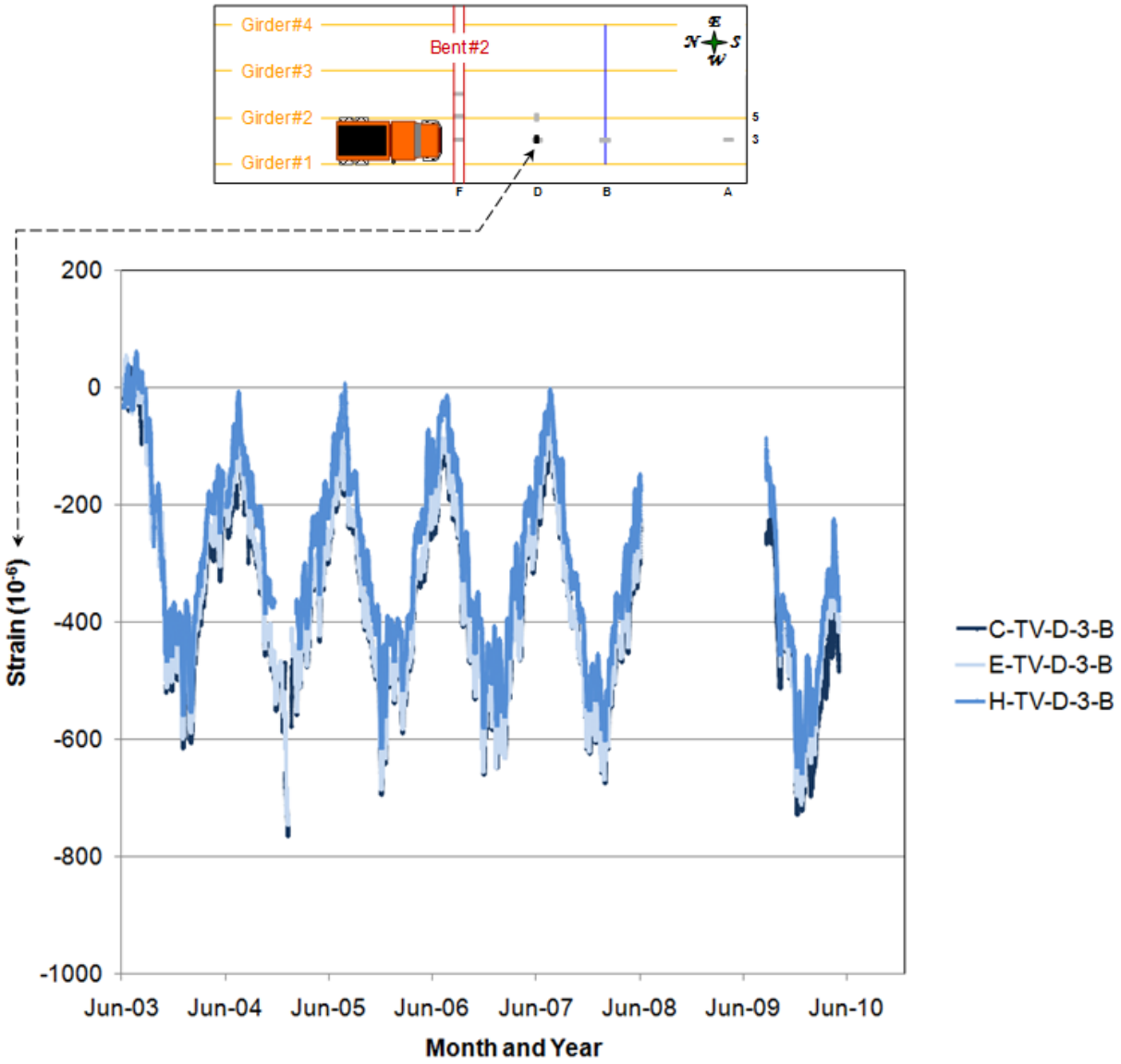

Figure B-4: Smoothed, transverse strain history at gage location D-3-B.

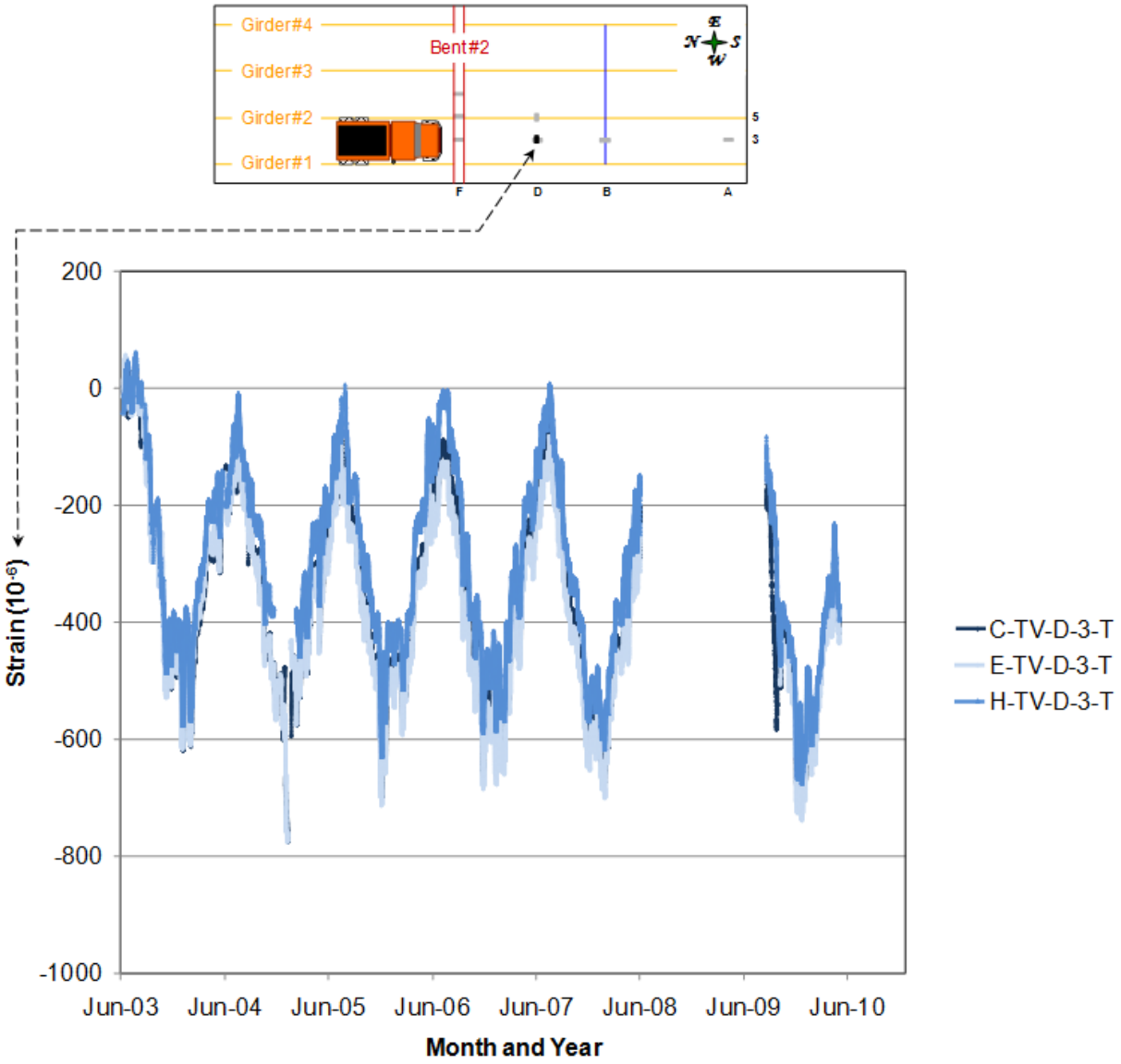

Figure B-5: Smoothed, transverse strain history at gage location D-3-T.

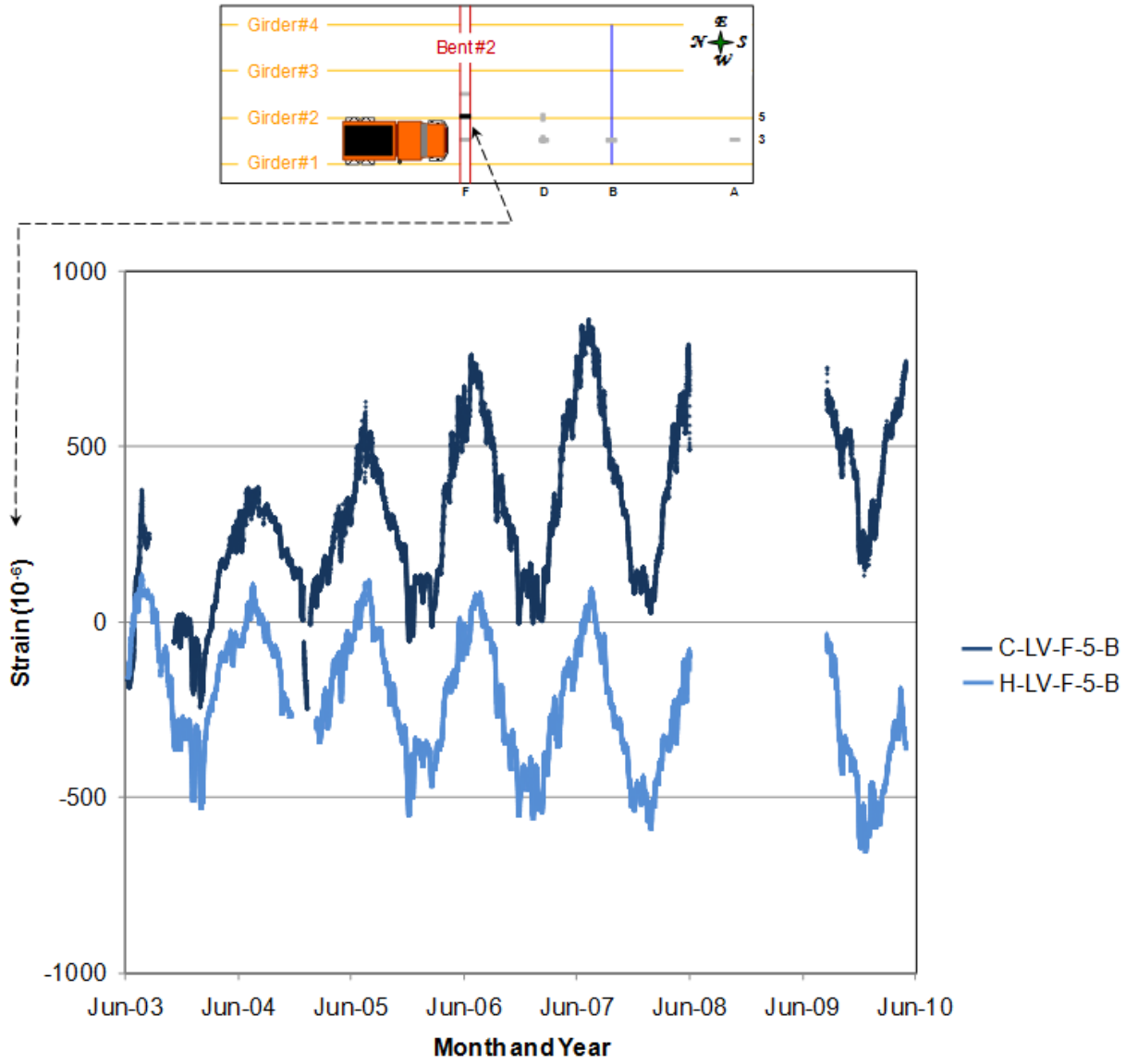

Figure B-6: Smoothed, longitudinal strain history at gage location F-5-B.

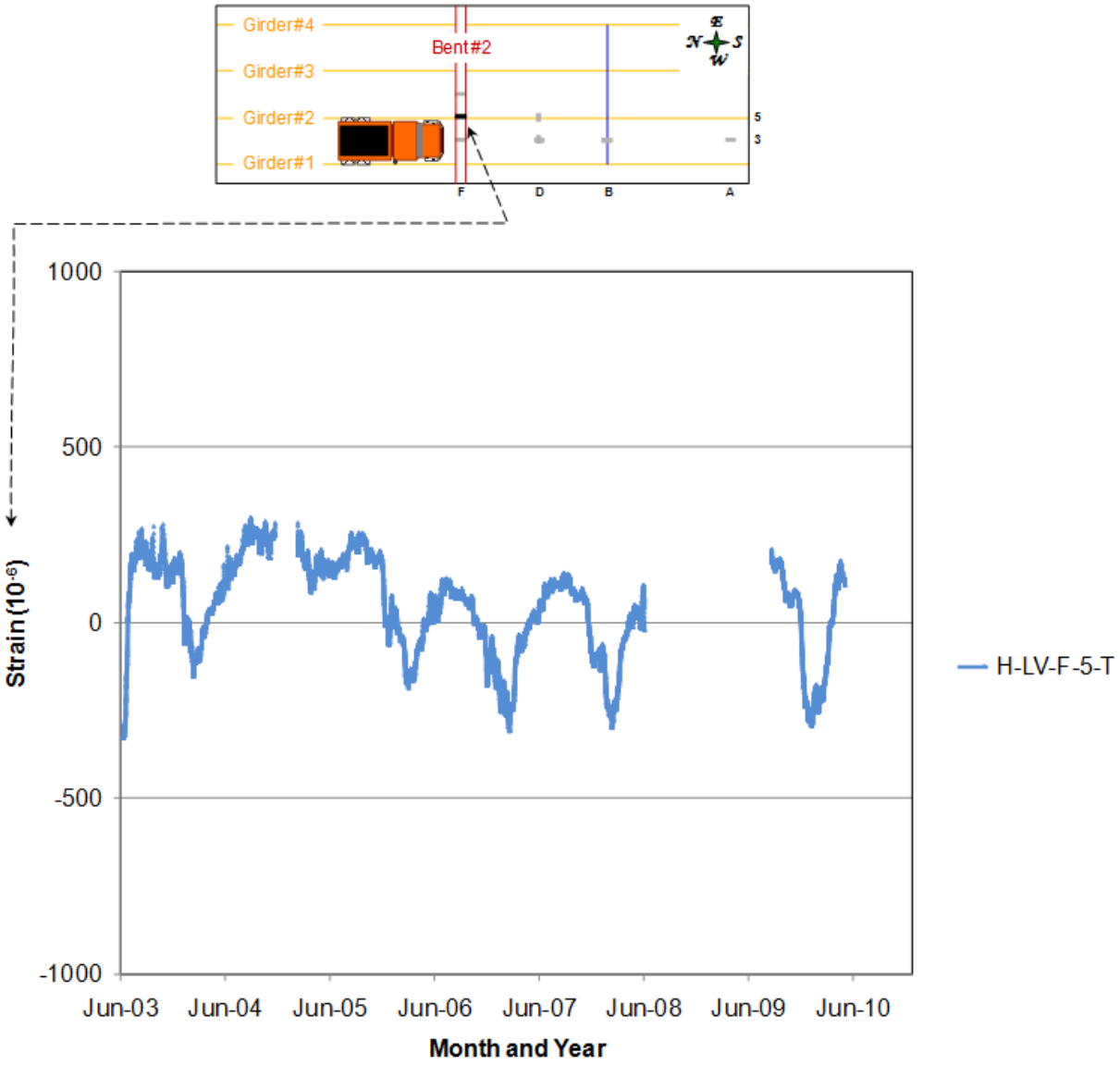

Figure B-7: Smoothed, longitudinal strain history at gage location F-5-T.

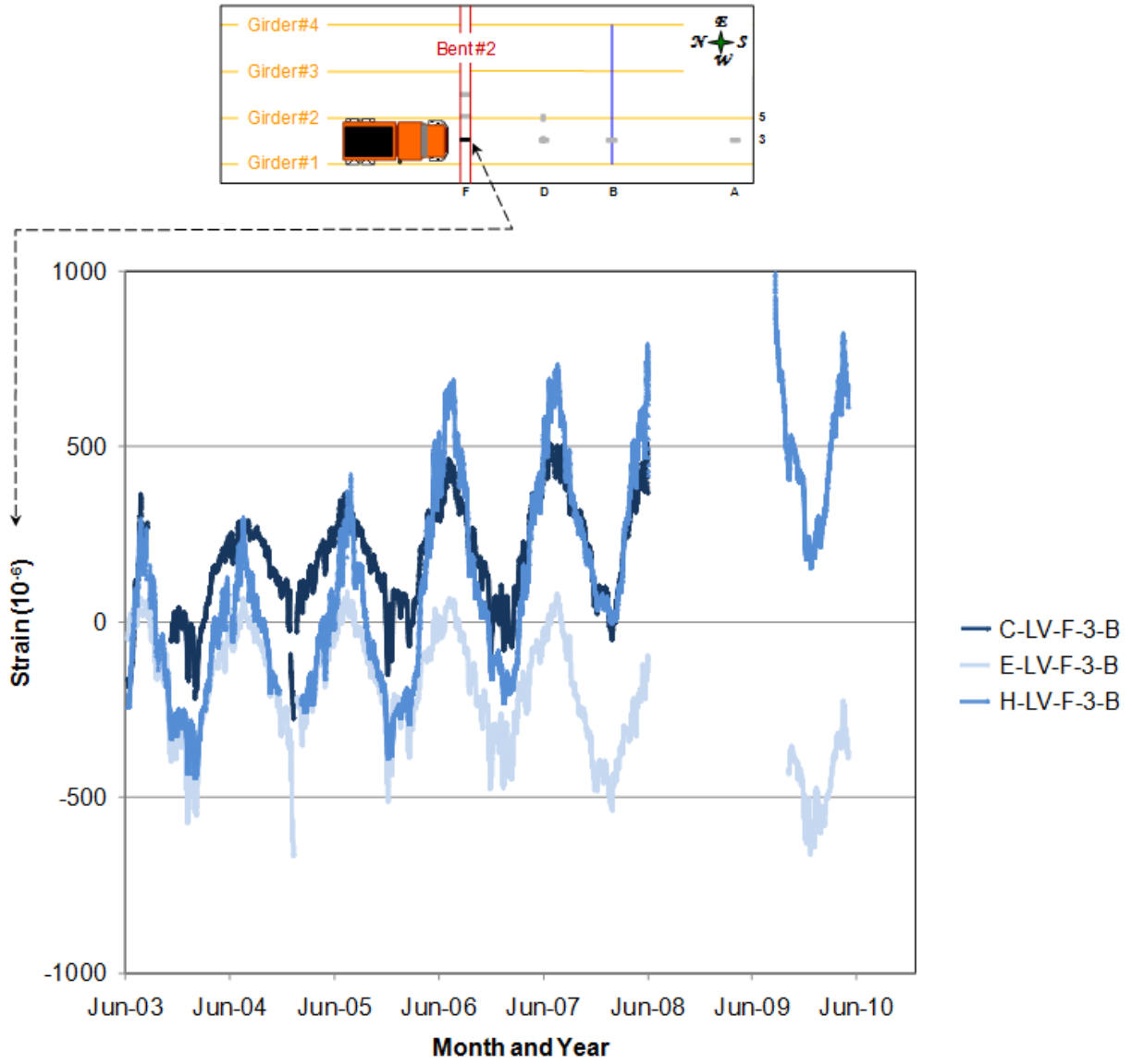

Figure B-8: Smoothed, longitudinal strain history at gage location F-3-B.

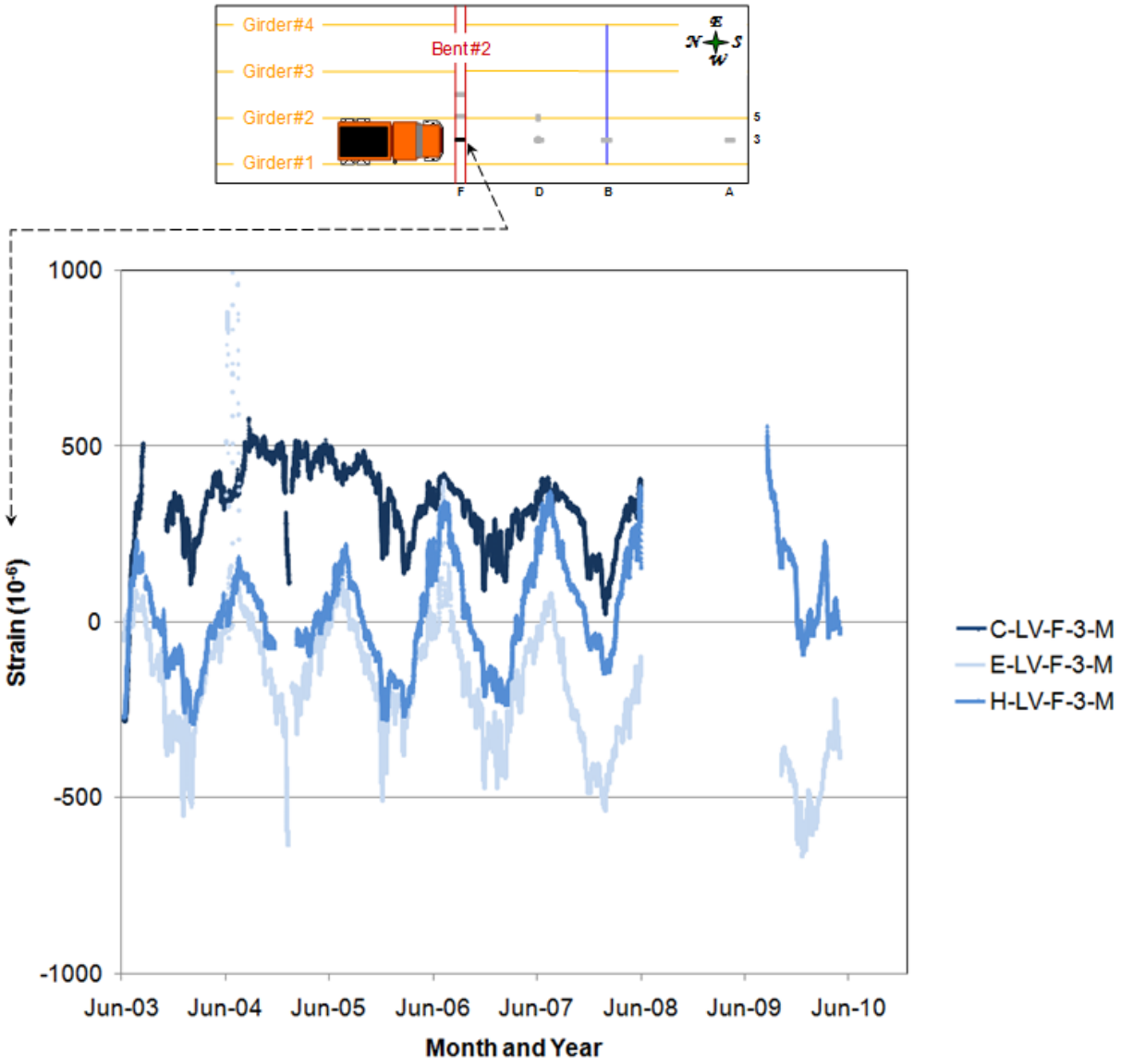

Figure B-9: Smoothed, longitudinal strain history at gage location F-3-M.

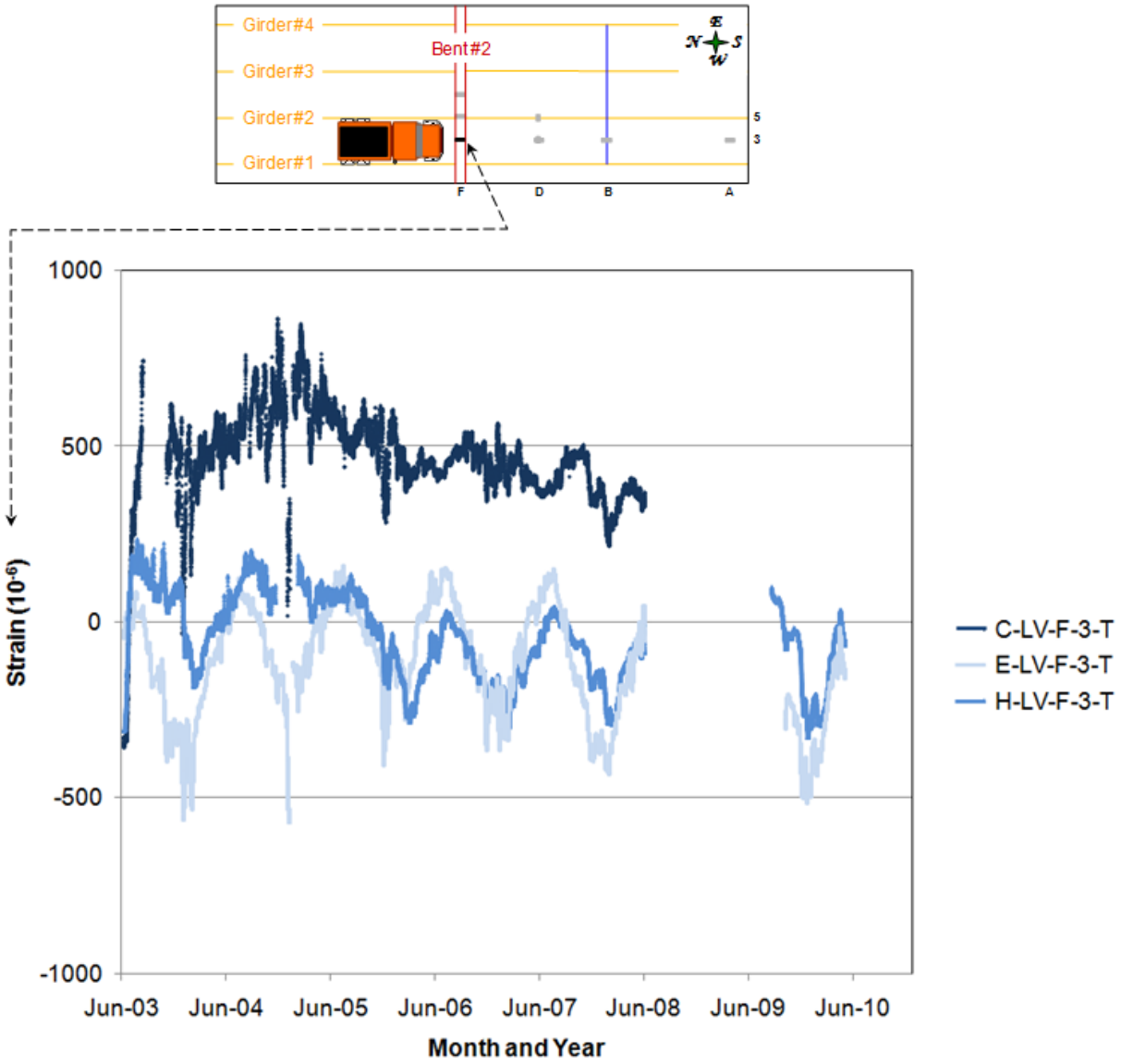

Figure B-10: Smoothed, longitudinal strain history at gage location F-3-T.

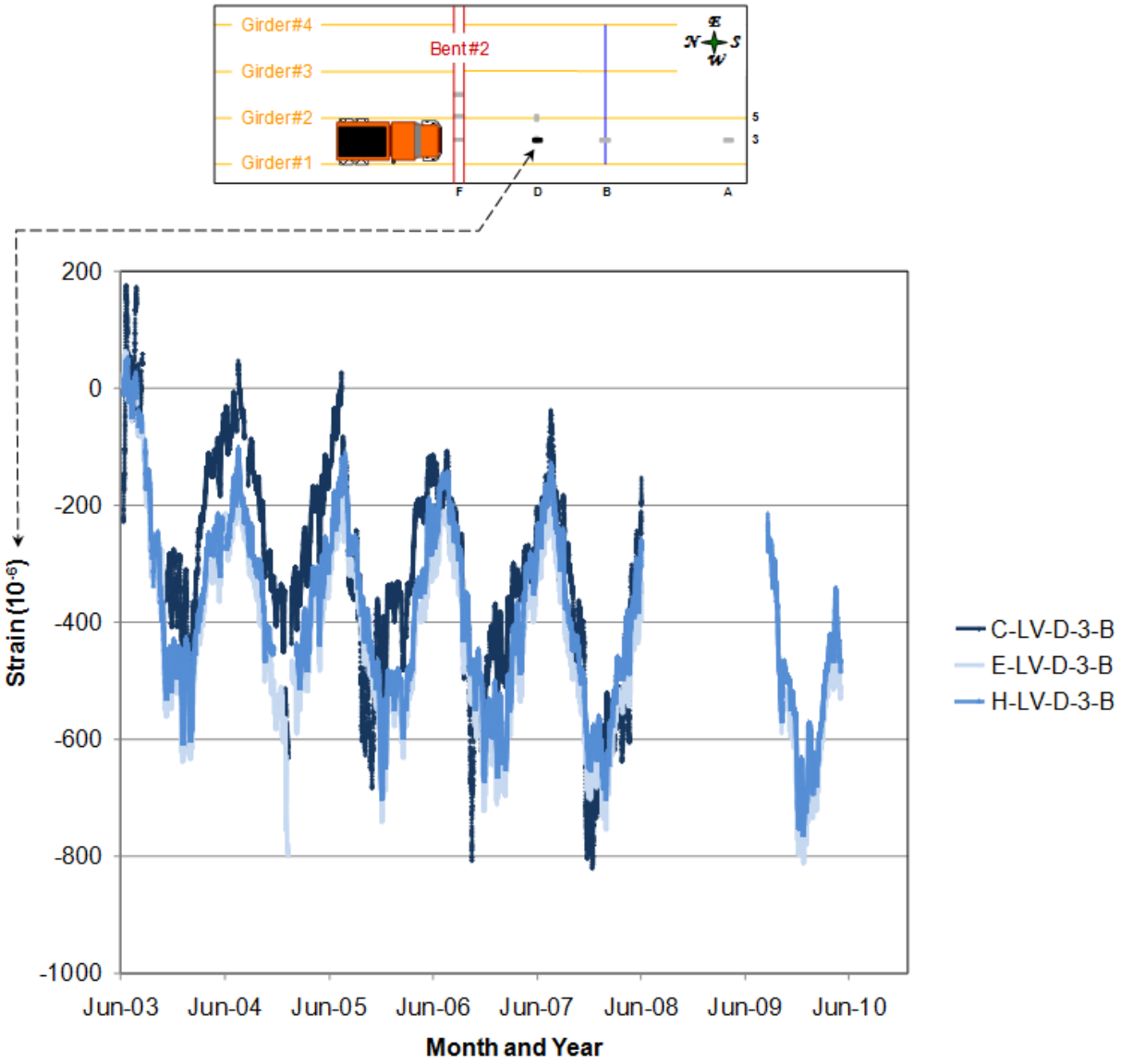

Figure B-11: Smoothed, longitudinal strain history at gage location D-3-B.

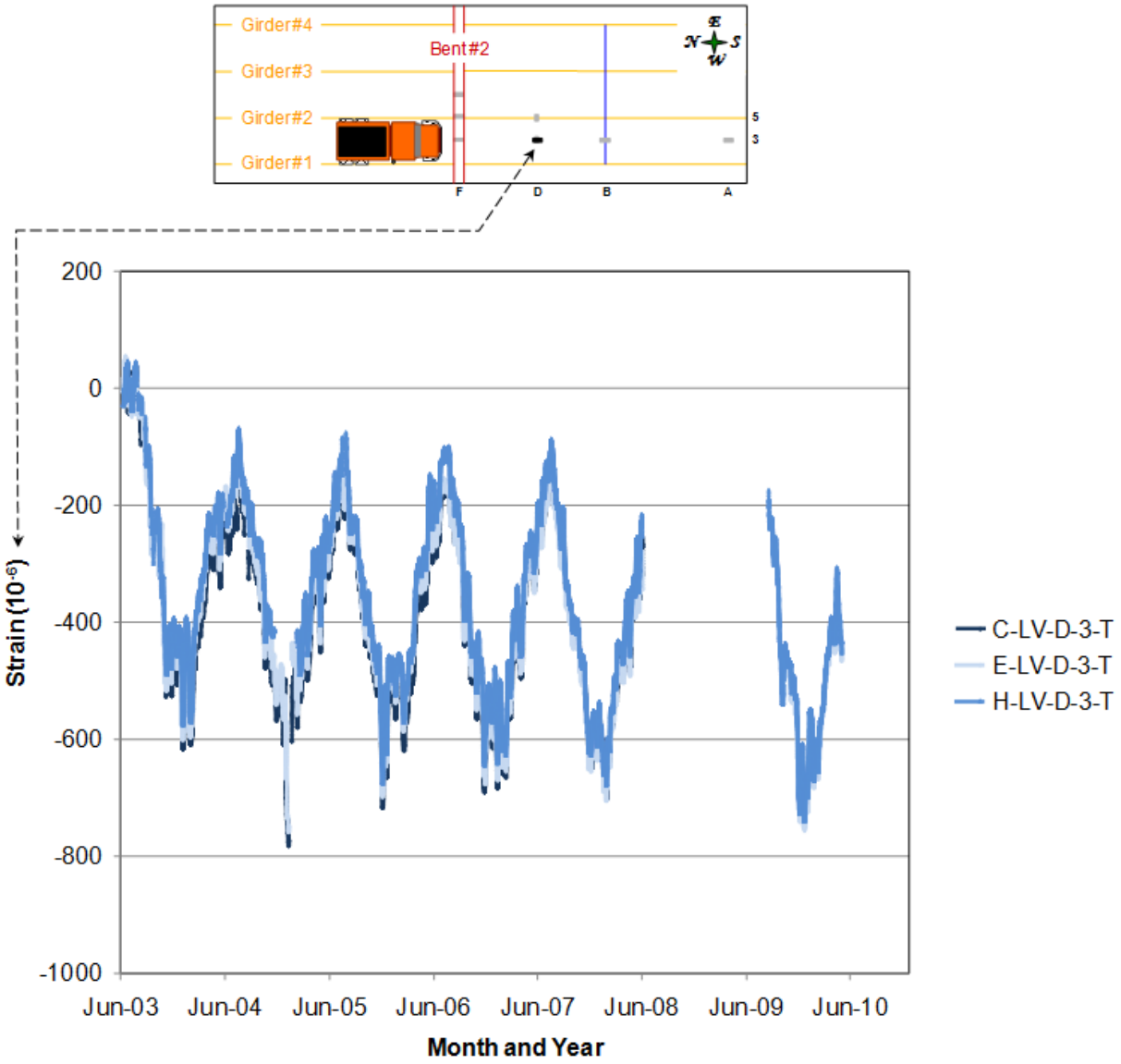

Figure B-12: Smoothed, longitudinal strain history at gage location D-3-T.

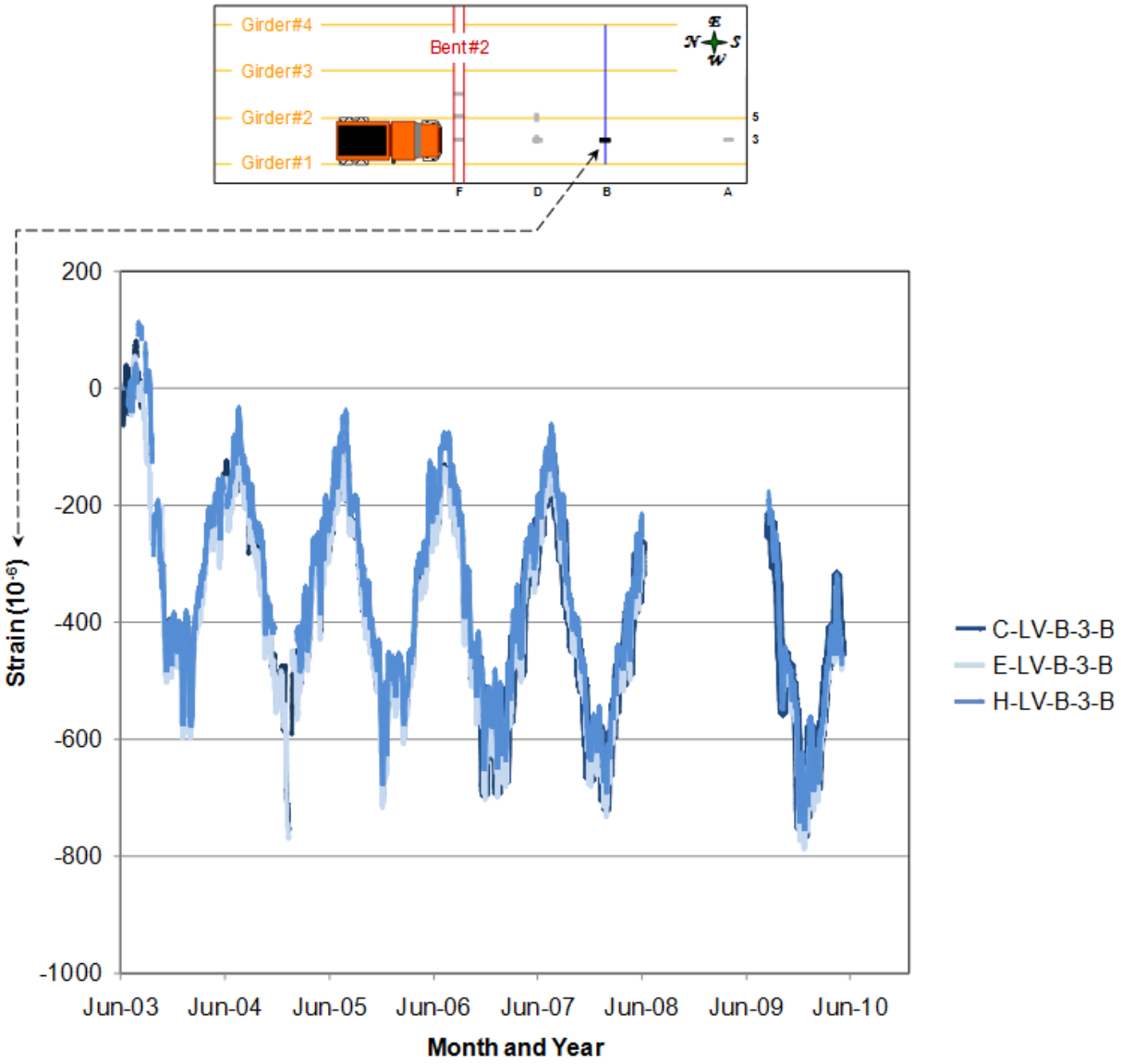

Figure B-13: Smoothed, longitudinal strain history at gage location B-3-B.

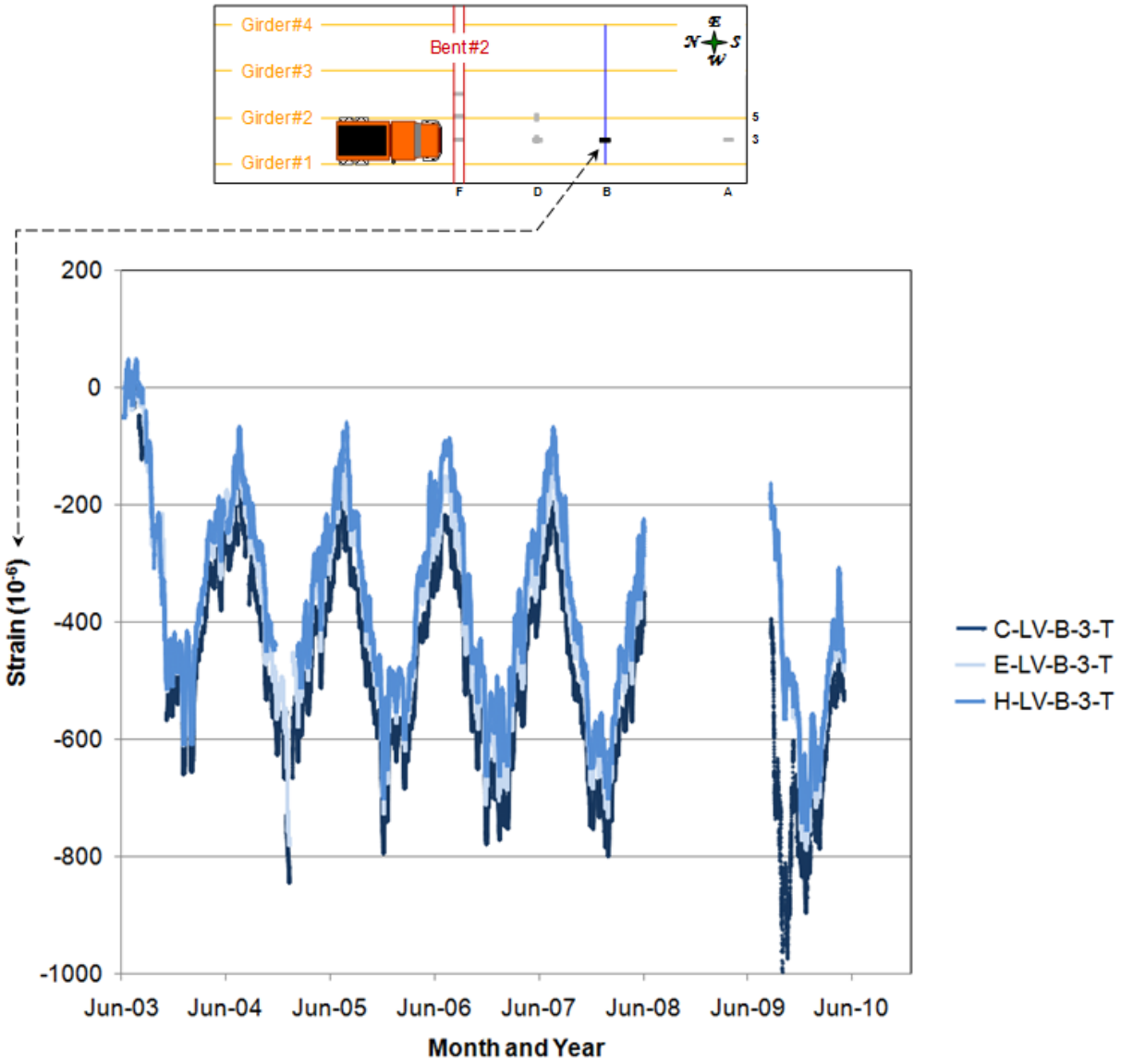

Figure B-14: Smoothed, longitudinal strain history at gage location B-3-T.

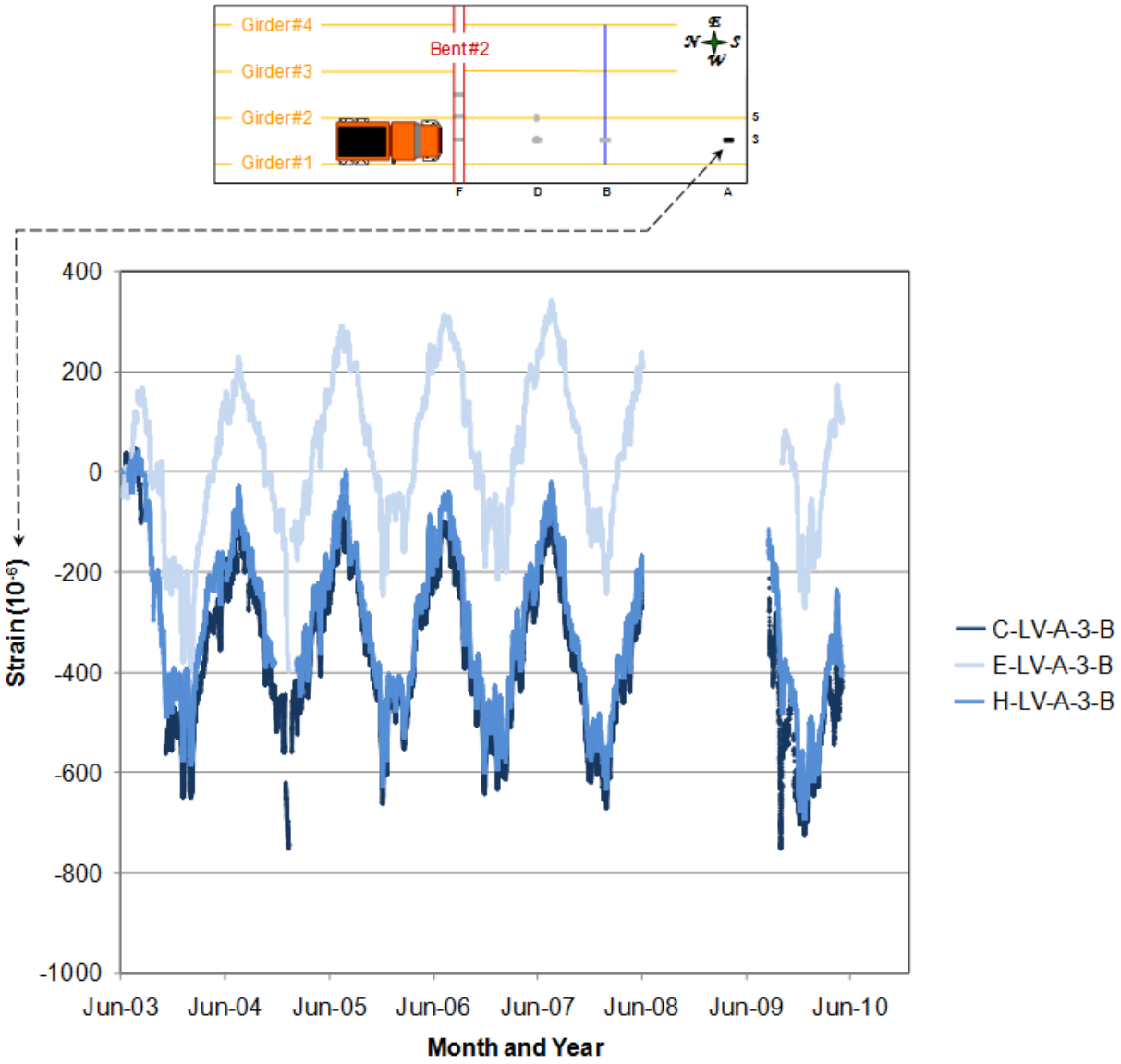

Figure B-15: Smoothed, longitudinal strain history at gage location A-3-B.

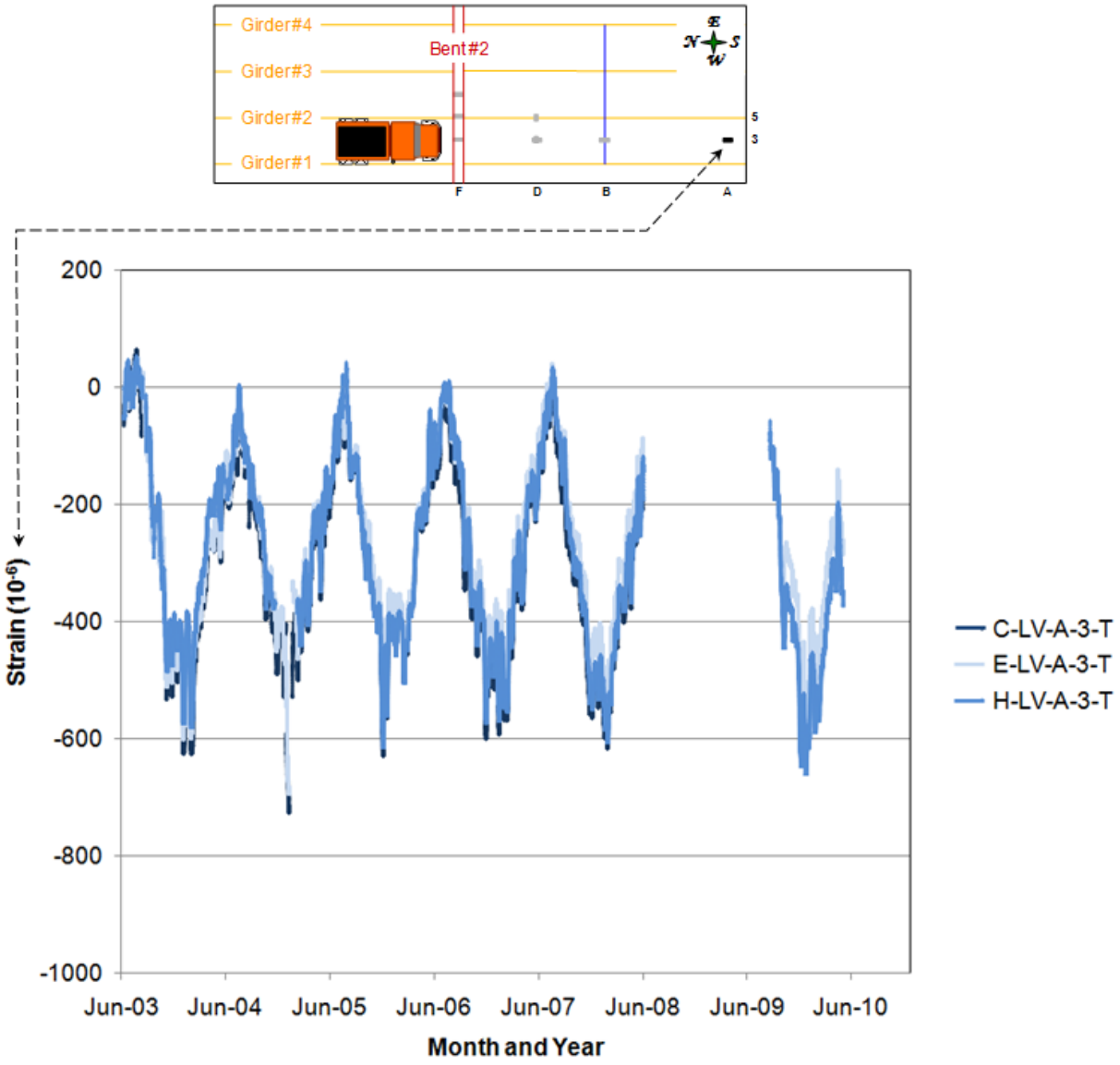

Figure B-16: Smoothed, longitudinal strain history at gage location A-3-T.

Appendix C:
Methodology and Results of Statistical Comparisons of Long-Term Strain Data

LIST OF TABLES

A statistical analysis of long term strain was used to reveal or verify any differences in behavior between the three bridge decks or over time. The total strain data for each gage (which included temperature effects) was used in the analysis. The methodologies and results of the analysis are elaborated on in more detail below; however, the implications of these results are discussed within the body of the report – not in this appendix.

Characterizing the overall response of the instrumented portions of the bridge decks was accomplished by averaging the strain responses from the vibrating wire strain gages. Comparisons between the raw strain responses obtained from these gages may also reveal differences in behavior between the three decks or between decks over time. While maximum and minimum strains are often used to characterize deck response, these values are more sensitive to anomalies. By calculating a mean response for each sensor, any potential inconsistencies will have less affect on the data, thus making comparisons between them more reliable. This methodology obviously masks true behavioral shapes of individual strain records, and therefore is used here for comparative purposes only, and not to characterize instantaneous deck behavior through time.

Variables that were investigated with respect to their influence on strain response were: deck type, time period (from Year 1 to Year 7, except Year 6), gage orientation (longitudinal versus transverse), and gage line (A, B, D, and F). Gage line F was not used in all the comparisons because obvious differences in strain between the bridges were seen along this gage line. Gage line F is located over the southern bent and strains detected by gages installed along this line are heavily influenced by the local response of the deck to the transverse cracks that developed there. The differences between the bridges at Gage line F are not representative of generalized bridge behavior.

The following procedure was used to get the data into a usable form. The strain record for each gage was parsed into selected time periods. The mean (μ_i) and standard deviation (s_i) were calculated using all of the data (consisting of n_i points) for a particular sensor and time period. The means and standard deviations for these individual sensors were then sorted based on the four criteria stated above (deck type, time period, gage orientation, and gage line). Equations C-1 and C-2 were used to calculate a combined mean (μ_T) and standard deviation (S_T) of a sorted group, respectively. In this case, N represents the number of data sets used to calculate the mean and not the number of data points. The combined coefficient of variation, V_T, was calculated using Equation C-3. Table C-1 through Table C-4 show the combined means of the strains for the various response groupings for each bridge.

$$\mu_T = \frac{\sum n_i \mu_i}{\sum n_i} \qquad \textbf{Equation C-1}$$

$$S_T^2 = \frac{1}{\sum n_i}\left[\sum\left(n_i s_i^2 + n_i \mu_i^2\right) - \sum n_i \mu_T^2\right] \qquad \textbf{Equation C-2}$$

$$V_T = \frac{S_T}{\mu_T} \qquad \textbf{Equation C-3}$$

In addition to mean strain response, the rate of change in the mean response over time was of interest. To determine this, the percent change between the strain response from a particular gage at two different time periods was computed (e.g., C-TV-A-3-B at a particular date and time in Year 1 compared to C-TV-A-3-B at that same date and time in Year 3). A single average value was then calculated from the thousands of values generated from these individual computations, along with the standard deviation. The following comparisons of the rates of change were made: Year 1 to Year 3, Year 3 to Year 7, and Year 1 to Year 7. The date and time between November 7 and May 6 were used within Years 1, 3 and 7. The resulting combined mean strains are shown in Table C-5.

Individual means were compared to one another using a two-sample, two-sided t-test. As discussed in the body of the report, the results from this test can be used to determine the p-value, which is an indicator that the means are similar. P-values range between zero and one, with p-values closer to zero indicating that the means are statistically less similar to one another and p-values closer to one indicating that the means are statistically more similar to one another. Table C-6 through Table C-10 report the statistical results (in the form of p-values) from the analysis. Relevant implications of these results are elaborated on in further detail within the body of the report.

Table C-1: Combined Means by Direction—All Time Periods, All Gage Lines Except F

Orientation	Bridge	Mean	St. dev.	COV	N
Longitudinal	**CON**	-385	199	-52	34
	EMP	-310	234	-75	36
	HPC	-353	177	-50	36
Transverse	**CON**	-368	183	-50	23
	EMP	-391	175	-45	30
	HPC	-318	174	-55	30

Table C-2: Combined Means by Gage Line—All Time Periods, Longitudinal Only

Line	Bridge	Mean	St. dev.	COV	N
A	**CON**	-337	174	-52	11
	EMP	-116	221	-190	12
	HPC	-307	173	-56	12
B	**CON**	-440	181	-41	12
	EMP	-400	176	-44	12
	HPC	-368	180	-49	12
D	**CON**	-373	228	-61	11
	EMP	-415	166	-40	12
	HPC	-384	168	-44	12
F	**CON**	334	327	98	29
	EMP	-72	544	-756	24
	HPC	-22	255	-1184	30

Table C-3: Combined Means by Year and Direction—All Gage Lines Except F

Orientation	Year	Bridge	Mean	St. dev.	COV	N
Longitudinal	1	CON	-352	189	-54	6
		EMP	-280	192	-69	6
		HPC	-306	174	-57	6
	2	CON	-301	141	-47	6
		EMP	-240	186	-77	6
		HPC	-259	125	-48	6
	3	CON	-361	176	-49	6
		EMP	-296	227	-77	6
		HPC	-345	159	-46	6
	4	CON	-390	190	-49	6
		EMP	-312	247	-79	6
		HPC	-348	177	-51	6
	5	CON	-414	212	-51	6
		EMP	-325	258	-79	6
		HPC	-373	181	-49	6
	7	CON	-624	204	-33	4
		EMP	-446	235	-53	6
		HPC	-517	129	-25	6
Transverse	1	CON	-349	173	-50	4
		EMP	-320	178	-56	5
		HPC	-293	172	-59	5
	2	CON	-313	136	-44	4
		EMP	-321	133	-41	5
		HPC	-237	128	-54	5
	3	CON	-364	180	-50	4
		EMP	-393	161	-41	5
		HPC	-315	159	-50	5
	4	CON	-368	201	-55	4
		EMP	-405	177	-44	5
		HPC	-304	180	-59	5
	5	CON	-377	193	-51	4
		EMP	-412	183	-44	5
		HPC	-324	182	-56	5
	7	CON	-486	139	-29	3
		EMP	-525	124	-24	5
		HPC	-465	125	-27	5

Table C-4: Combined Means by Gage Line and Year—Longitudinal Only

Line	Year	Bridge	Mean	St. dev.	COV	N
A	1	CON	-373	184	-49	2
		EMP	-193	201	-104	2
		HPC	-294	174	-59	2
	2	CON	-277	117	-42	2
		EMP	-74	179	-242	2
		HPC	-221	123	-56	2
	3	CON	-305	158	-52	2
		EMP	-93	218	-235	2
		HPC	-294	158	-54	2
	4	CON	-330	172	-52	2
		EMP	-88	233	-265	2
		HPC	-295	176	-60	2
	5	CON	-346	180	-52	2
		EMP	-88	238	-271	2
		HPC	-315	179	-57	2
	7	CON	-550	150	-27	1
		EMP	-196	208	-106	2
		HPC	-458	126	-28	2
B	1	CON	-372	165	-44	2
		EMP	-311	173	-55	2
		HPC	-302	180	-59	2
	2	CON	-350	128	-36	2
		EMP	-313	124	-39	2
		HPC	-264	124	-47	2
	3	CON	-421	160	-38	2
		EMP	-392	155	-40	2
		HPC	-361	158	-44	2
	4	CON	-448	175	-39	2
		EMP	-418	170	-41	2
		HPC	-366	176	-48	2
	5	CON	-466	179	-39	2
		EMP	-435	176	-40	2
		HPC	-395	181	-46	2
	7	CON	-613	175	-28	2
		EMP	-569	121	-21	2
		HPC	-547	120	-22	2
D	1	CON	-310	206	-67	2
		EMP	-337	169	-50	2
		HPC	-322	168	-52	2
	2	CON	-267	139	-52	2
		EMP	-334	122	-36	2
		HPC	-290	119	-41	2
	3	CON	-356	190	-53	2
		EMP	-404	145	-36	2
		HPC	-379	147	-39	2
	4	CON	-391	204	-52	2
		EMP	-429	158	-37	2
		HPC	-383	165	-43	2
	5	CON	-431	254	-59	2
		EMP	-452	165	-36	2
		HPC	-408	168	-41	2
	7	CON	-776	286	-37	1
		EMP	-573	117	-20	2
		HPC	-545	119	-22	2

Table C-5: Combined Means by Direction and Age—Percent Change

Orientation	Year*	Bridge	Mean	St. dev.	COV	N
Longitudinal	1 to 3	CON	32	33	104	2
		EMP	28	32	115	2
		HPC	30	40	135	2
	3 to 7	CON	19	28	148	2
		EMP	19	23	127	2
		HPC	23	28	122	2
	1 to 7	CON	55	43	78	2
		EMP	49	34	70	2
		HPC	55	49	89	2
Transverse	1 to 3	CON	16	34	217	3
		EMP	24	36	151	3
		HPC	16	32	198	3
	3 to 7	CON	14	36	250	3
		EMP	10	27	275	3
		HPC	18	31	174	3
	1 to 7	CON	28	44	156	3
		EMP	32	37	116	3
		HPC	30	32	104	3

* November 7 to May 6 within each time period

Table C-6: P-values, Comparisons Between Decks by Direction—All Time Periods, All Gage Lines Except F

Orientation	Comparison	P-value
Longitudinal	CON-EMP	0.157
	CON-HPC	0.487
	EMP-HPC	0.386
Transverse	CON-EMP	0.653
	CON-HPC	0.310
	EMP-HPC	0.109

Table C-7: P-values, Comparisons Between Decks by Gage Line—All Time Periods, Longitudinal Only

Line	Comparison	P-value
A	CON-EMP	0.015
	CON-HPC	0.690
	EMP-HPC	0.029
B	CON-EMP	0.581
	CON-HPC	0.337
	EMP-HPC	0.668
D	CON-EMP	0.614
	CON-HPC	0.894
	EMP-HPC	0.648
F	CON-EMP	0.003
	CON-HPC	0.000
	EMP-HPC	0.678

Table C-8: P-values, Comparisons Between Decks by Direction and Year—All Gage Lines except F

Orientation	Year	Comparison	P-value
Longitudinal	1	CON-EMP	0.533
		CON-HPC	0.673
		EMP-HPC	0.815
	2	CON-EMP	0.540
		CON-HPC	0.597
		EMP-HPC	0.845
	3	CON-EMP	0.595
		CON-HPC	0.871
		EMP-HPC	0.680
	4	CON-EMP	0.554
		CON-HPC	0.701
		EMP-HPC	0.777
	5	CON-EMP	0.531
		CON-HPC	0.727
		EMP-HPC	0.720
	7	CON-EMP	0.246
		CON-HPC	0.405
		EMP-HPC	0.539
Transverse	1	CON-EMP	0.814
		CON-HPC	0.647
		EMP-HPC	0.814
	2	CON-EMP	0.931
		CON-HPC	0.427
		EMP-HPC	0.342
	3	CON-EMP	0.809
		CON-HPC	0.681
		EMP-HPC	0.463
	4	CON-EMP	0.779
		CON-HPC	0.636
		EMP-HPC	0.398
	5	CON-EMP	0.789
		CON-HPC	0.690
		EMP-HPC	0.470
	7	CON-EMP	0.713
		CON-HPC	0.845
		EMP-HPC	0.471

Table C-9: P-values, Comparisons Between Decks By Gage Line and Year—Longitudinal Only

Line	Year	Comparison	P-value
A	1	CON-EMP	0.521
		CON-HPC	0.733
		EMP-HPC	0.688
	2	CON-EMP	0.408
		CON-HPC	0.726
		EMP-HPC	0.513
	3	CON-EMP	0.465
		CON-HPC	0.955
		EMP-HPC	0.482
	4	CON-EMP	0.447
		CON-HPC	0.871
		EMP-HPC	0.500
	5	CON-EMP	0.436
		CON-HPC	0.893
		EMP-HPC	0.475
	7	CON-EMP	—
		CON-HPC	—
		EMP-HPC	0.371
B	1	CON-EMP	0.779
		CON-HPC	0.755
		EMP-HPC	0.969
	2	CON-EMP	0.816
		CON-HPC	0.618
		EMP-HPC	0.762
	3	CON-EMP	0.883
		CON-HPC	0.771
		EMP-HPC	0.878
	4	CON-EMP	0.890
		CON-HPC	0.722
		EMP-HPC	0.815
	5	CON-EMP	0.891
		CON-HPC	0.761
		EMP-HPC	0.858
	7	CON-EMP	0.816
		CON-HPC	0.734
		EMP-HPC	0.886
D	1	CON-EMP	0.908
		CON-HPC	0.959
		EMP-HPC	0.943
	2	CON-EMP	0.696
		CON-HPC	0.884
		EMP-HPC	0.779
	3	CON-EMP	0.822
		CON-HPC	0.914
		EMP-HPC	0.890
	4	CON-EMP	0.870
		CON-HPC	0.971
		EMP-HPC	0.822
	5	CON-EMP	0.937
		CON-HPC	0.933
		EMP-HPC	0.836
	7	CON-EMP	—
		CON-HPC	—
		EMP-HPC	0.852

Table C-10: P-values, Comparisons Between Decks by Age—Percent Change

Orientation	Year*	Comparison	P-value
Longitudinal	1 to 3	CON-EMP	0.922
		CON-HPC	0.957
		EMP-HPC	0.973
	3 to 7	CON-EMP	0.999
		CON-HPC	0.902
		EMP-HPC	0.894
	1 to 7	CON-EMP	0.901
		CON-HPC	0.992
		EMP-HPC	0.900
Transverse	1 to 3	CON-EMP	0.782
		CON-HPC	0.987
		EMP-HPC	0.788
	3 to 7	CON-EMP	0.866
		CON-HPC	0.907
		EMP-HPC	0.750
	1 to 7	CON-EMP	0.915
		CON-HPC	0.951
		EMP-HPC	0.954

* November 7 to May 6 within each time period

This public document was published in electronic format at no cost.